



2010-09

Consolidation of surface coatings by friction stir techniques

Young, Jeremiah J.

Monterey, California. Naval Postgraduate School

<http://hdl.handle.net/10945/5180>



Calhoun is a project of the Dudley Knox Library at NPS, furthering the precepts and goals of open government and government transparency. All information contained herein has been approved for release by the NPS Public Affairs Officer.

Dudley Knox Library / Naval Postgraduate School
411 Dyer Road / 1 University Circle
Monterey, California USA 93943

<http://www.nps.edu/library>



**NAVAL
POSTGRADUATE
SCHOOL**

MONTEREY, CALIFORNIA

THESIS

**CONSOLIDATION OF SURFACE COATINGS BY
FRICTION STIR TECHNIQUES**

by

Jeremiah J. Young

September 2010

Thesis Advisor:	Terry R. McNelley
Second Reader:	Sarath Menon

Approved for public release; distribution is unlimited

THIS PAGE INTENTIONALLY LEFT BLANK

REPORT DOCUMENTATION PAGE		Form Approved OMB No. 0704-0188	
Public reporting burden for this collection of information is estimated to average 1 hour per response, including the time for reviewing instruction, searching existing data sources, gathering and maintaining the data needed, and completing and reviewing the collection of information. Send comments regarding this burden estimate or any other aspect of this collection of information, including suggestions for reducing this burden, to Washington headquarters Services, Directorate for Information Operations and Reports, 1215 Jefferson Davis Highway, Suite 1204, Arlington, VA 22202-4302, and to the Office of Management and Budget, Paperwork Reduction Project (0704-0188) Washington DC 20503.			
1. AGENCY USE ONLY (Leave blank)		2. REPORT DATE September 2010	3. REPORT TYPE AND DATES COVERED Master's Thesis
4. TITLE AND SUBTITLE Consolidation of Surface Coatings by Friction Stir Techniques		5. FUNDING NUMBERS	
6. AUTHOR(S) Jeremiah J. Young		8. PERFORMING ORGANIZATION REPORT NUMBER	
7. PERFORMING ORGANIZATION NAME(S) AND ADDRESS(ES) Naval Postgraduate School Monterey, CA 93943-5000		10. SPONSORING/MONITORING AGENCY REPORT NUMBER	
9. SPONSORING /MONITORING AGENCY NAME(S) AND ADDRESS(ES) N/A		11. SUPPLEMENTARY NOTES The views expressed in this thesis are those of the author and do not reflect the official policy or position of the Department of Defense or the U.S. Government. IRB Protocol number N/A.	
12a. DISTRIBUTION / AVAILABILITY STATEMENT Approved for public release; distribution is unlimited		12b. DISTRIBUTION CODE A	
13. ABSTRACT Friction Stir Processing (FSP) is an emerging technology that allows for the processing of regions near the surface of a material in order to improve upon the existing mechanical properties. Aluminum alloy samples were plasma sprayed with a Titanium-Nickel-Chrome coating or a Titanium coating. Single and multiple pass experiments were performed with both a pinned and a pinless FSP tool at rotation speeds of 400, 800 and 1500 revolutions per minute; all traverses were done at four inches per minute. Optical and electron microscopy methods were then used to determine the success at consolidating the relatively hard and porous Titanium based coatings onto the Aluminum alloy surface. Results showed that the most successful results were accomplished using a flat, pinless tool, with minimal downward force applied to the sample. The Titanium coatings were visibly less porous at microscopic levels, and there was also considerably less separation at the coating-base interface. Energy dispersive x-ray spectroscopy showed very little mixing of the base material and the plasma sprayed coating.			
14. SUBJECT TERMS Friction Stir Processing, Aluminum 7075, Surface Coating, Surface Consolidation.			15. NUMBER OF PAGES 79
			16. PRICE CODE
17. SECURITY CLASSIFICATION OF REPORT Unclassified	18. SECURITY CLASSIFICATION OF THIS PAGE Unclassified	19. SECURITY CLASSIFICATION OF ABSTRACT Unclassified	20. LIMITATION OF ABSTRACT UU

NSN 7540-01-280-5500

Standard Form 298 (Rev. 2-89)
Prescribed by ANSI Std. Z39-18

THIS PAGE INTENTIONALLY LEFT BLANK

Approved for public release; distribution is unlimited

**CONSOLIDATION OF SURFACE COATINGS BY FRICTION STIR
TECHNIQUES**

Jeremiah J. Young
Lieutenant, United States Navy
B.S., University of Kansas, 2005

Submitted in partial fulfillment of the
requirements for the degree of

MASTER OF SCIENCE IN MECHANICAL ENGINEERING

from the

**NAVAL POSTGRADUATE SCHOOL
September 2010**

Author: Jeremiah J. Young

Approved by: Terry R. McNelley
Thesis Advisor

Sarath Menon
Second Reader

Knox T. Millsaps
Chairman, Department of Mechanical and
Aerospace Engineering

THIS PAGE INTENTIONALLY LEFT BLANK

ABSTRACT

Friction Stir Processing (FSP) is an emerging technology that allows for the processing of regions near the surface of a material in order to improve upon the existing mechanical properties. Aluminum alloy samples were plasma sprayed with a Titanium-Nickel-Chrome coating or a Titanium coating. Single and multiple pass experiments were performed with both a pinned and a pinless FSP tool at rotation speeds of 400, 800 and 1500 revolutions per minute, all traverses were done at four inches per minute. Optical and electron microscopy methods were then used to determine the success at consolidating the relatively hard and porous Titanium based coatings onto the Aluminum alloy surface. Results showed that the most successful results were accomplished using a flat, pinless tool, with minimal downward force applied to the sample. The Titanium coatings were visibly less porous at microscopic levels, and there was also considerably less separation at the coating-base interface. Energy dispersive x-ray spectroscopy showed very little mixing of the base material and the plasma sprayed coating.

THIS PAGE INTENTIONALLY LEFT BLANK

TABLE OF CONTENTS

I.	INTRODUCTION	1
II.	BACKGROUND INFORMATION	9
A.	FRICITION STIR PROCESSING	9
B.	ALUMINUM 7075	9
C.	TITANIUM PLASMA SPRAY	11
III.	EXPERIMENTAL PROCEDURE	15
A.	OVERVIEW	15
B.	MATERIAL PROCESSING AND PREPARATION	15
C	MICROSTRUCTURE ANALYSIS	20
1.	Optical Microscopy	20
a.	<i>Sample Preparation</i>	20
b.	<i>Optical Microscopy Procedure</i>	22
2.	Scanning Electron Microscope	22
a.	<i>Sample Preparation</i>	22
b.	<i>Scanning Electron Microscopy Procedure</i> ..	22
3.	Hardness Data	24
IV.	RESULTS	27
A.	OVERVIEW	27
B.	AS PLASMA SPRAYED SAMPLE CHARACTERISTICS	27
C.	MICROSCTRUCTURE ANALYSIS	31
1.	Optical Microscopy	31
2.	Scanning Electron Microscope	35
D.	HARDNESS DATA	46
V.	DISCUSSION	49
VI.	CONCLUSIONS	53
VII.	RECOMMENDATIONS FOR FUTURE WORK	55
	LIST OF REFERENCES	57
	INITIAL DISTRIBUTION LIST	59

THIS PAGE INTENTIONALLY LEFT BLANK

LIST OF FIGURES

Figure 1.	Schematic of FSW. From [1].....	3
Figure 2.	Schematic of FSW. From [2].....	5
Figure 3.	Schematic of the different zones that are produced as a result of FSW. From [2].....	6
Figure 4.	Plasma spray facility and schematic. From [13]...	12
Figure 5.	Arcing of helicopter blade leading edges in contact with debris in the air, in this case, sand. From [14].....	13
Figure 6.	Arcing of helicopter leading edges erodes protective metal layer leaving the blades vulnerable to excessive pitting and further erosion. From [14].....	14
Figure 7.	Threaded Pin Used in FSP shown inserted into traversing device. From [15].....	16
Figure 8.	Flat tools I, II, and III.....	17
Figure 9.	Ti-Ni-Cr coated sample. A: Single pass FSP, B: Multiple pass FSP, I: Flat pinless tool, II: Pinless tool with small nub, III: Pinless tool with large nub; (The discoloration on spots II and III are due to tool failure).....	18
Figure 10.	Titanium coated sample showing FSP; D,E: pinned tool single pass FSP, C: Pinless tool FSP; notice the resultant flash on run E. Excessive force led to removal of all Titanium from the surface.....	19
Figure 11.	Friction stir processing machinery. From [7]...	20
Figure 12.	TOPCOM Field Emission SEM.....	23
Figure 13.	Zeiss Neon 40 Field Emission SEM.....	24
Figure 14.	Harness testing machine.....	25
Figure 15.	SEM image of plasma sprayed Titanium. Notice the evident voids that form as a result of uneven distribution of material to the surface. Such voids lead to an inherently weaker, and thus, poorly bonded outer layer.....	28
Figure 16.	Inconsistent Titanium coating (light gray) leaves the base Aluminum (dark gray) exposed, thereby defeating the purpose of the protective coating. (The very light color at the top is the puck used to mount the sample).....	29
Figure 17.	The thickest part of coating measured at over 150 microns; yet the visible voids and cracking at the interface will undoubtedly lead to an overall weaker protective layer.....	30

Figure 18.	Cracks and pores present before processing contribute to the poor bonding at the interface of the two metals, as well as weakening to the protective coating.....	31
Figure 19.	FSP stir zone A, single pass, pinned tool sample.....	32
Figure 20.	FSP stir zone B, multi-pass, pinned tool sample.....	32
Figure 21.	Unprocessed sample shows a random distribution grain structure that is not refined.....	33
Figure 22.	Top to bottom: Non FSP region, edge of SZ, middle of SZ; All photos at the same magnification. Notice the Stir Zone's superior mixing and more homogeneous microstructure.....	34
Figure 23.	Stir Zone A: Secondary electron image (top) showing that there is very little or no Titanium coating on the surface of the sample in the stir zone area. Xray spectrum from the area marked + in the image shown (bottom). There is no evidence of Titanium in the region. Titanium K_{α} line is expected at 4.51keV.....	36
Figure 24.	Stir zone B secondary electron image (top, taken in the vicinity of the + on the image) shows some consolidation between the broken up Titanium particles (light gray) and the base Aluminum (dark gray). Xray spectrum (bottom) shown the expected 4.51keV Titanium K_{α} line.....	38
Figure 25.	Stir zone D: The dark base is the Aluminum, the lighter the Titanium; Notice the barley present titanium is no longer on the surface as protection.....	39
Figure 26.	SEM photo of plunge area I; The lighter "white" material is the Titanium, while the darker Aluminum base makes up the majority of material.....	41
Figure 27.	EDS data of plunge area I; Titanium still present on the surface.....	41
Figure 28.	As cast Aluminum-Silicon alloy micrograph.....	42
Figure 29.	1500 RPM plunge showing the intact Titanium layer and the much improved porosity, with very little mixing of the Titanium and Aluminum.....	43
Figure 30.	SZ of the flat tool FSP run shows much less porosity that the as plasma sprayed sample or the pinned FSP experiments. Along with reduced porosity, there is very little evident separation at the Titanium-Aluminum interface...	45

- Figure 31. Line scan of the flat tool FSP run; Aluminum shown in red, Titanium shown in Green. The line scan shows in addition to reducing porosity and minimizing cracks at the interface, very little mixing occurs between the Titanium and the Aluminum, demonstrating successful treatment of the surface layer while minimally affecting the base metal.....46
- Figure 32. A graph of Vickers hardness vs Depth (in mm). As expected, FSP of a metal leads to increased hardness, partly by refining and homogenizing the microstructure. Increased hardness was observed in both the Titanium and the Aluminum..47
- Figure 33. Scanning electron image of: Single pass (left) versus multiple pass (right) surface consolidation. The multipass mixing is far superior and yields a more homogenized particle distribution. (Light gray particles are the Titanium).....49
- Figure 34. Scanning electron image of: Unprocessed material before (left) and after (right) flat tool FSP. FSP material consistently shows reduced porosity, less cracking at the interface, and a more even Titanium distribution along the surface.....50

THIS PAGE INTENTIONALLY LEFT BLANK

LIST OF TABLES

Table 1.	Composition of Aluminum 7075; Note: value is maximum if range not shown. From [12].....	11
Table 2.	List of sandpaper grit and machine RPM.....	21

THIS PAGE INTENTIONALLY LEFT BLANK

LIST OF ACRONYMS AND ABBREVIATIONS

Al	Aluminum
AL7075	Aluminum Alloy 7075
Cr	Chromium
EDM	Electric Discharge Machine
EDS	Energy Dispersive X-Ray Spectroscopy
FSP	Friction Stir Processing
FSW	Friction Stir Welding
HAZ	Heat Affected Zone
SEM	Scanning Electron Microscope
SiC	Silicon Carbide
SZ	Stir Zone
TMAZ	Thermo=Mechanically Affected Zone
Ti	Titanium
TWI	The Welding Institute

THIS PAGE INTENTIONALLY LEFT BLANK

ACKNOWLEDGMENTS

I would like to thank Professor McNelley for allowing me to join this project. His patience and guidance allowed for me to grow professionally and to achieve the best results possible in my education.

I would like to extend a very special thank you to Professor Sarath Menon. No single individual had a greater impact on my master's education than him. His expertise in the classroom and in the laboratory greatly enhanced my knowledge and appreciation for the work that he so often helped me with. Thank you for your education expertise, tutelage, and guidance over the last two years. I was lucky to have my career path cross yours for such a time.

Also, I would like to thank Will Young. Thanks for the numerous times you dropped what you were doing to help me fix the problem of that day. Your door was always open to me, and your assistance was truly appreciated. Good luck with your studies.

Perhaps most important, I need to thank my family. To my loving wife, Stacey, I thank you for understanding how important this degree was to me. Thank you for the sacrifices you made to accommodate my school work, and the support you offered when I became overwhelmed. To my daughters, Mackenzie and Kaitlynn, one day you will see why I had to study so much, and why I will expect you to do the same.

THIS PAGE INTENTIONALLY LEFT BLANK

I. INTRODUCTION

Friction Stir processing (FSP) is an emerging technology used to improve the material properties of a metal, and lately, attention has been placed on this method as a means to consolidate coatings into a base metal. Aluminum is by nature much softer and less wear resistant than other metals, such as steel, but has a much lower density and a higher strength-to-weight ratio in bending. Aluminum has many uses in the U.S. Navy and aerospace industries but is prone to erosion and pitting when exposed to harsh environments. If coated with a much harder metal, such as titanium, nickel or chrome, one can take advantage of the inherent material properties of aluminum, while greatly reducing the disadvantages of wear and erosion. There are several techniques available to coat metals with other metals, but all have shortcomings. This investigation of Titanium coated Aluminum samples begins with a poorly bonded porous coating that is extremely inconsistent in depth. The goal of using FSP would be to close up the porosities, increase the bonding strength of the Titanium to the base Aluminum, and to refine the microstructure, possibly increasing the hardness at the surface. One can accomplish this via mixing that occurs during the processing of the coating and the base. Ideally, one is left with a very fine microstructure that contains small grains of Titanium that are well bonded at the surface.

FSP is a technique based on the success of friction stir welding (FSW). FSW was invented at The Welding

Institute (TWI), located in Cambridge, United Kingdom, in 1991. FSW is a solid-state welding technique that has the capability to weld without using an arc or melting either of the metals involved. The welding is accomplished via a hardened rotating tool that is plunged into abutting edges of the two metals. The metals to be joined must be clamped in place on an anvil. The rotating tool plastically deforms the metals in the weld zone (WZ), heating the material and then traverses along the butted edges. Since the welding occurs below the melting temperature of both metals, no filler material is needed, resulting in little change in the weld chemical composition. The heating action of the rotating tool softens the metal, and as the tool is moved along the joint, material is mechanically forced from the front of the tool to the rear, forming the weld.

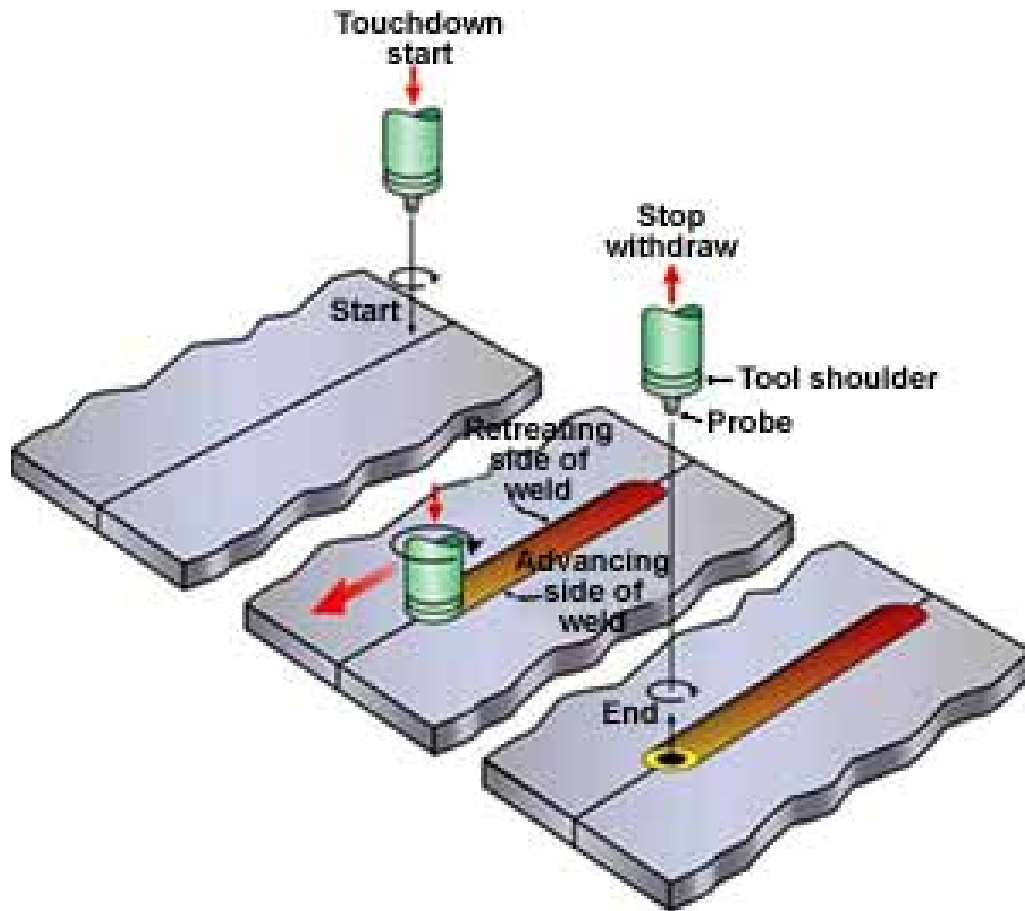


Figure 1. Schematic of FSW. From [1].

The FSP process is very similar to FSW, though joining is not involved. Instead, the main goal of FSP is to process a single metallic work piece so as to improve some characteristic of it by virtue of a refined microstructure, and/or a consolidated, well bonded protective coating. By modifying the existing microstructure, some of the results can include: increased hardness, increased strength, increased ductility, and reduced porosity.

The microstructure is changed via FSP in a manner very similar to FSW. A hardened rotating tool is inserted into the metal and traversed in a predetermined pattern, and then removed. The tool is usually cylindrical in shape and

often has a pin protruding from the bottom end (pinned) or can be relatively flat on the bottom end (pinless). The tool must be made from a very hard material so as to prevent wear particles from the tool from entering the work piece. Pin tools have a shoulder at the top of the pin to restrict material movement in the upward direction, ensuring that the material may only travel around the pin during deformation. Once the tool is completely inserted into the metal to be processed, it is traversed along a desired path, which need not be linear. The volume of material defined by the path on which the pin has traversed, and the pin depth, is referred to as the stir zone (SZ). Outside the SZ is the thermo mechanically affected zone (TMAZ), so named because although less stirring has taken place in the TMAZ, the material properties are usually altered. Outside the TMAZ is the Heat affected Zone (HAZ). The HAZ is identified because even though no stirring has taken place, the material properties may have been altered due to exposure to heat that the stirring action has produced. Thus it is standard practice to identify the SZ, TMAZ and HAZ for FSP material. A piece of metal may undergo FSP once, referred to as single-pass, or more than once, usually referred to as multi-pass FSP.

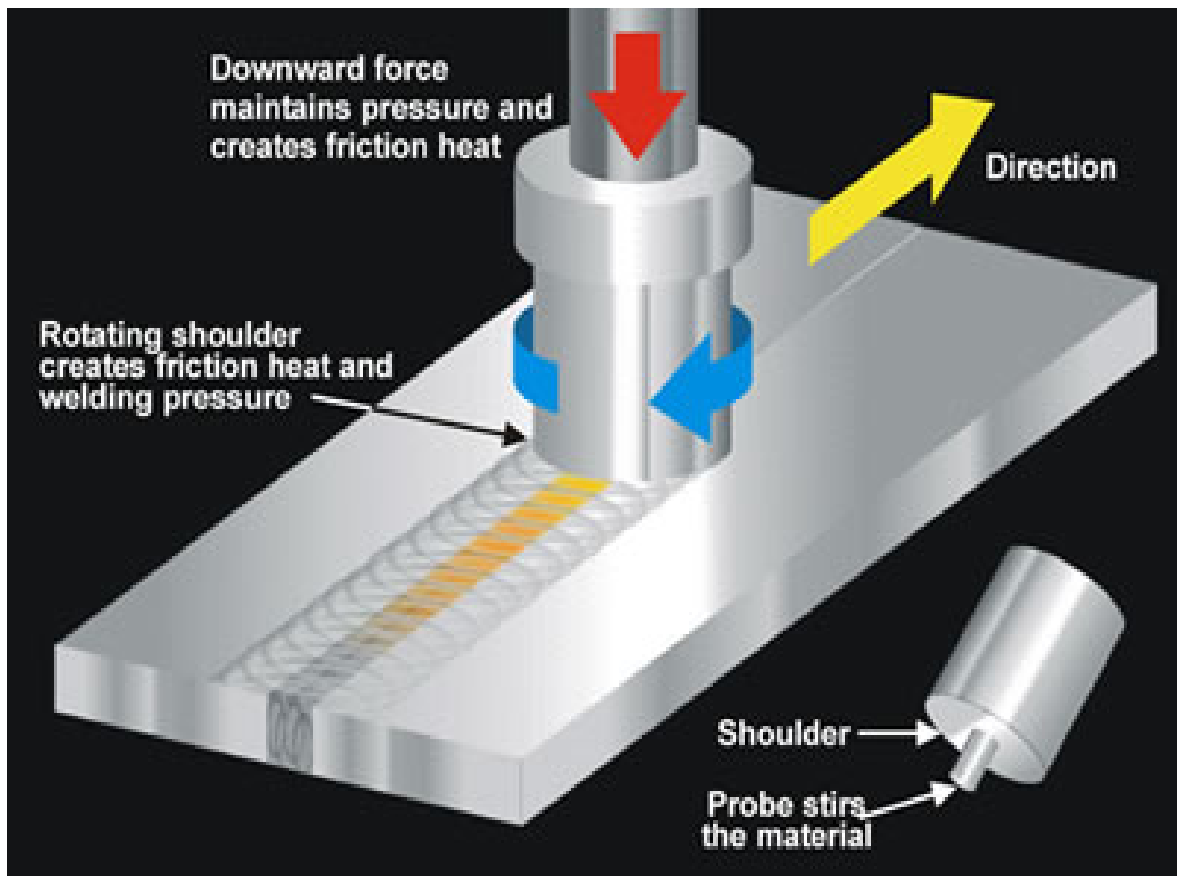


Figure 2. Schematic of FSW. From [2].

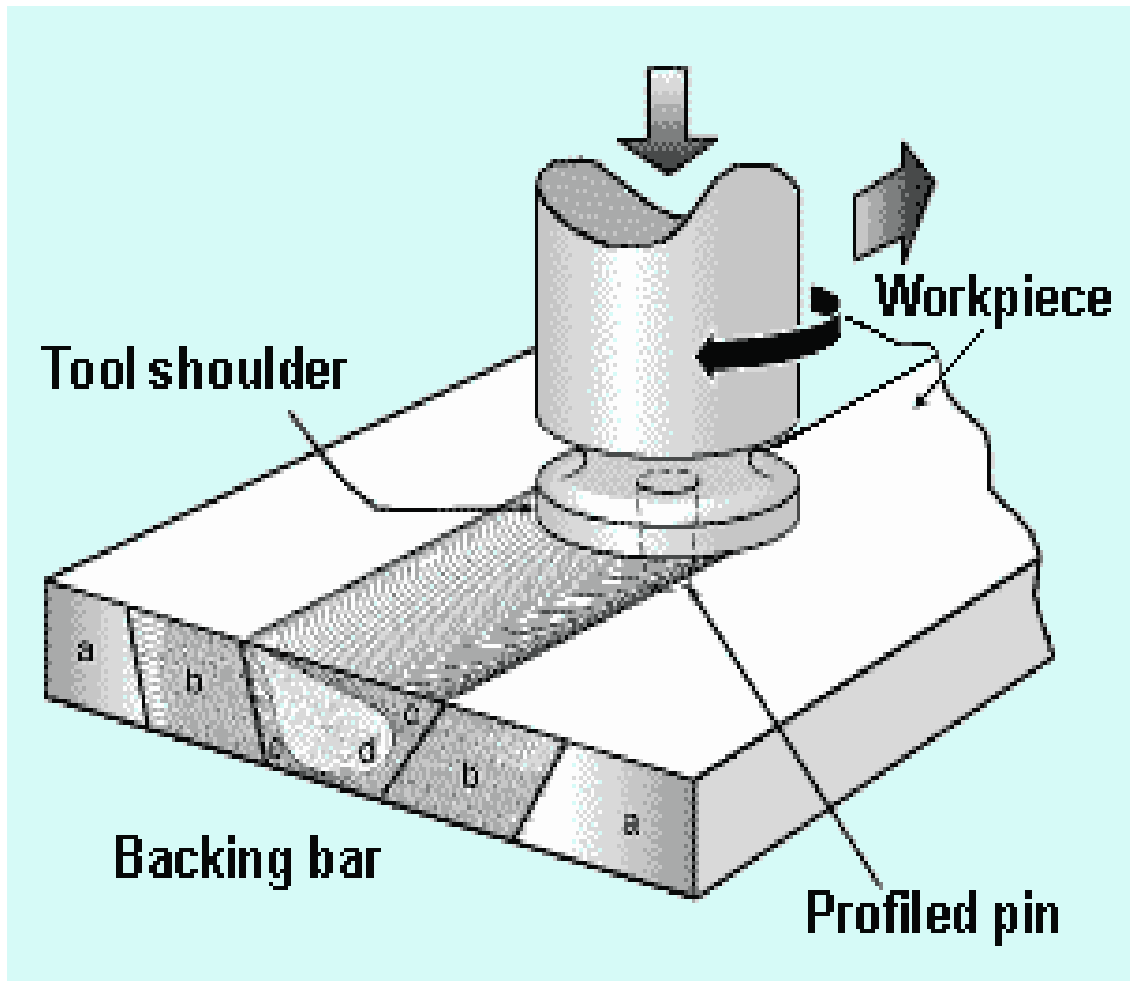


Figure 3. Schematic of the different zones that are produced as a result of FSW. From [2].

Figure 3 shows the various labeled zones in a piece of FSW metal: 'a' represents the unaffected material, 'b' shows the HAZ, 'c' shows the TMAZ, and 'd' shows the weld nugget. If the metal were instead FSP, region d would be labeled as the stir zone. The other areas would remain the same.

In the short time that FSP has been available, many useful FSP techniques have been discovered, as well as many advantages over conventional welding or processing techniques:

Compared to metalworking techniques, FSP has distinct advantages. First, FSP is a short-route, solid-state processing technique with one-step processing that achieves micro structure refinement, densification, and homogeneity. Second, the microstructure and mechanical properties of the processed zone can be accurately controlled by optimizing the tool design, FSP parameters and active cooling/heating. Third, the depth of the processed zone can be optimally designed by changing the length of the tool pin with the depth being between several hundred micrometers and tens of millimeters; it is difficult to achieve an optimally design process depth with other metalworking techniques. Fourth, FSP is a versatile technique with a comprehensive function for the fabrication, processing, and synthesis of materials. Fifth, the heat input during FSP comes from friction and plastic deformation, which means FSP is a green and energy efficient technique without deleterious gas, irradiation, and noise. Sixth, FSP does not change the shape and size of the processed components [3].

These advantages highlight the important aspects about the friction stir process, the desired characteristics of such a process, as well as the unique results that can be accomplished.

THIS PAGE INTENTIONALLY LEFT BLANK

II. BACKGROUND INFORMATION

A. FRICTION STIR PROCESSING

Because of the difficulty of fusion welding concerning aluminum, FSW and FSP offer a very reliable alternative to conventional welding and metal treatment methods. Although FSP and FSW have been shown to be successful on other metals, aluminum alloys comprise the majority of the metals to utilize these techniques.

FSP of aluminum-based alloys has been the object of several recent experiments in the last decade and have shown to be very successful in many areas. Such examples include: Modification of surface treatments to increase hardness [4], modification of microstructure so as to achieve very fine grain evolution [5],[6], enhancing mechanical properties of cast Aluminum alloys [7], evolution of high strain rate superplasticity [8], as well as others[9],[10].

Conventionally, a pinned tool has been used to FSP a metal, but recently there have been investigations into the possibility of a pinless tool. In 2009, a group of researchers were able to achieve superior consolidation of a powder coating with a base metal, increasing hardness at the surface by nearly twenty five percent [4].

B. ALUMINUM 7075

Aluminum was chosen as the base metal due to its extensive list of applications, as well as its inherent mechanical properties. Aluminum alloy 7075 (Al7075) is often used in transport applications, including marine,

automotive and aviation applications, due to its high strength-to-density ratio. Its strength and light weight are also desirable in other fields. Rock climbing equipment, bicycle components, and hang glider airframes are commonly made from 7075 aluminum alloy. One interesting use for 7075 is in the manufacture of M16 rifle parts for the American military. Due to its strength, low density, thermal properties and its ease of polishing, 7075 is widely used in mould tool manufacture. This alloy has been further refined into other 7000 series alloys for this application namely 7050 and 7020 [11].

Aluminum 7075 is typically comprised of the following alloying elements, listed in weight percentage:

Chemical Composition of Alloys	
Element	Weight % for Al 7075
Si	.4
Fe	.5
Cu	1.2-2.0
Mn	.3
Mg	2.1-2.9
Cr	.18-.28
Zn	5.1
Ti	.2
Others, each	.5
Others, total	.15

Al	Balance
----	---------

Table 1. Composition of Aluminum 7075; Note: value is maximum if range not shown. From [12].

C. TITANIUM PLASMA SPRAY

When using the plasma spray technique, a material is introduced into a plasma jet, which in turn originates from a plasma torch, as shown in Figure 4. The material to be used as a coating can be a powder or liquid. The coating material can attain very high temperatures, upwards of 10,000K while in the plasma jet, and is then propelled towards the substrate. Upon deposition, the molten droplets are flattened and solidify very quickly, forming the coating. The deposited flattened particles, commonly referred to as splats, take shape as the droplets, then cool and harden. The thickness of the deposited splats is usually only a few microns, while the length and width may be up to one hundred microns. Because of the shape of the splats there tend to be regions of voids, cracks, and poor bonding. As mentioned earlier, the primary purposes of plasma coating a metal is to protect against high temperatures, corrosion, erosion, and wear.

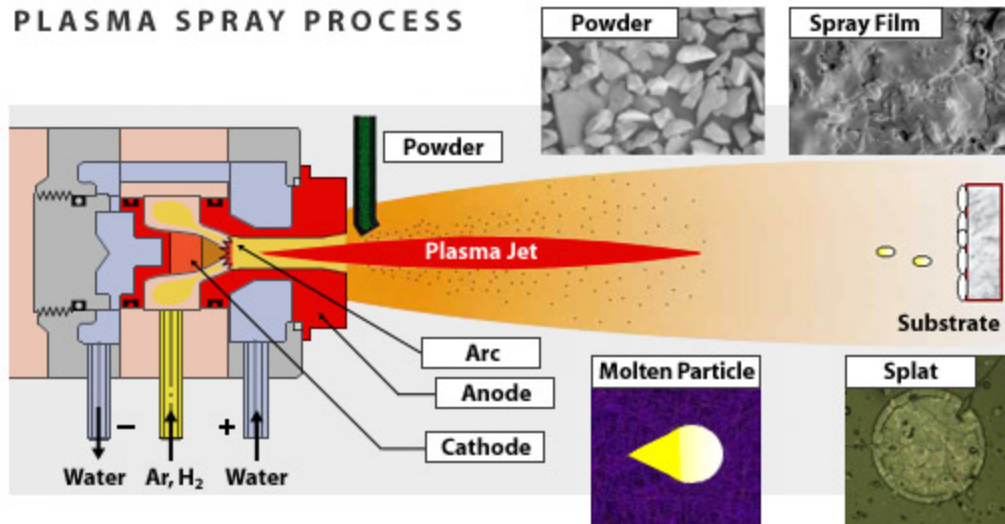


Figure 4. Plasma spray facility and schematic. From [13].

There are often cracks present both in the Titanium coating, and also along the Titanium-Aluminum interface. These cracks most certainly lead to the flaking and loss of the outer layer due to the lack of bonding, especially when the coating is exposed to fast moving debris. As the Titanium breaks off, the base Aluminum is left exposed to the environment. Harsh conditions will then pit and erode a soft metal such as Aluminum, leading to more repair and upkeep to components, such as helicopter blade leading edges, while lowering the usability of the aircraft due to an increased maintenance cycle.

Figures 5 and 6 show helicopters conducting operations in the harsh environment of the Middle East. As the helicopter blades encounter airborne sand, several incendiary particles are seen. These fragments are believed to be the protective coating, applied to the leading edges of the blades, being removed by the collision with the sand. This phenomenon has not only been observed

during takeoff and landing, but also at higher altitudes, especially during sandstorms. In addition to the damage caused to the leading edges of the blades, this effect can be especially dangerous during night-time operations, as the incendiary halo can be visible for miles.



Figure 5. Arcing of helicopter blade leading edges in contact with debris in the air, in this case, sand. From [14].



Figure 6. Arcing of helicopter leading edges erodes protective metal layer leaving the blades vulnerable to excessive pitting and further erosion. From [14].

III. EXPERIMENTAL PROCEDURE

A. OVERVIEW

This research focuses on comparing the microstructural characteristics, interface bonding strength, and surface hardness of unprocessed Titanium coated Al-7075 to that which has undergone FSP. This was accomplished using optical microscopy and scanning electron microscopy, energy dispersive x-ray spectroscopy (EDS), as well as obtaining Vickers's hardness data.

B. MATERIAL PROCESSING AND PREPARATION

Four Aluminum plates, two Al7075 and two Aluminum-Silicon alloy plates were plasma sprayed with a Titanium based coatings at SRI International, courtesy of Dr. Angel Sanjuurjo. The feedstock for the plasma spray consisted of a 50% weight percentage mixture of Titanium sponge powder (-80+200 mesh) and a Nickel-Chromium-Iron alloy powder. In the second experiment, only Titanium sponge powder was used. The plasma sprayed samples were subsequently friction stir processed under a number of different conditions as described later. All plates have dimension of approximately 65 mm by 45 mm. The pinned tool FSP samples were prepared using an RPM of 800 and a traverse rate of 4 inches per minute. The pinned tool had a pin 3 mm in length and 3 mm in diameter. The shoulder diameter was 10 mm. The first set of pinless tool plunges was done with an RPM of 800, and had a shoulder diameter of 12.0 mm. The second round of plunges was conducted at 400, 800, and 1500 RPM, using the same tools from the first set. The pinless flat tool traverse was accomplished at an RPM of

800, and an IPM of four inches per minute (101.6 mm/min). From these plates, several samples were sectioned using a computer-controlled Charmilles Andrew EF630 electric discharge machine (EDM) and a consumable brass cutting wire with a nominal diameter of .30 mm. All samples were cut and sectioned such that the transverse plane, normal to the direction of tool travel, could be analyzed.

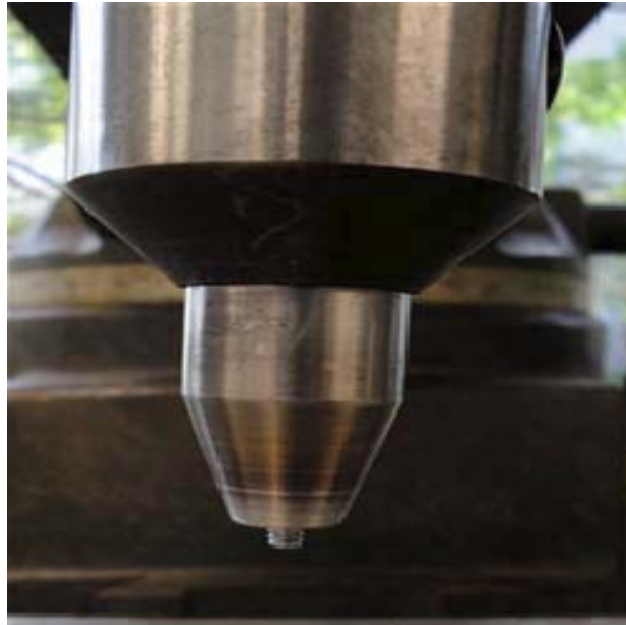


Figure 7. Threaded Pin Used in FSP shown inserted into traversing device. From [15].



Figure 8. Flat tools I, II, and III.

Four separate types of FSP runs were made on the material: single pass with a pinned tool, multiple pass with a pinned tool, a pure plunge and removal using a pinless tool, and a traverse using a pinless tool. In order to preserve material, each piece of material saw more than one FSP pass, done with sufficient separation so as not to interfere with data concerning other passes. Figures 9 and 10 show the plates on which some of the experiments were conducted.

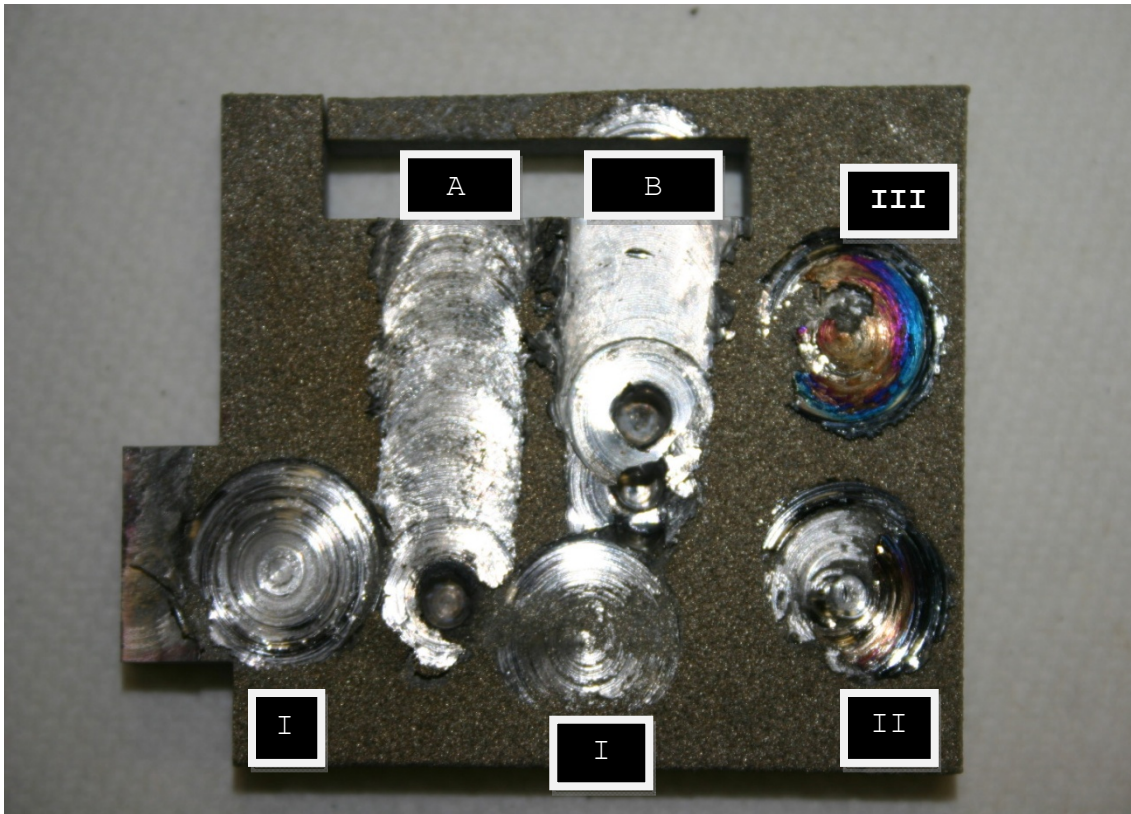


Figure 9. Ti-Ni-Cr coated sample. A: Single pass FSP, B: Multiple pass FSP, I: Flat pinless tool, II: Pinless tool with small nub, III: Pinless tool with large nub; (The discoloration on spots II and III are due to tool failure).

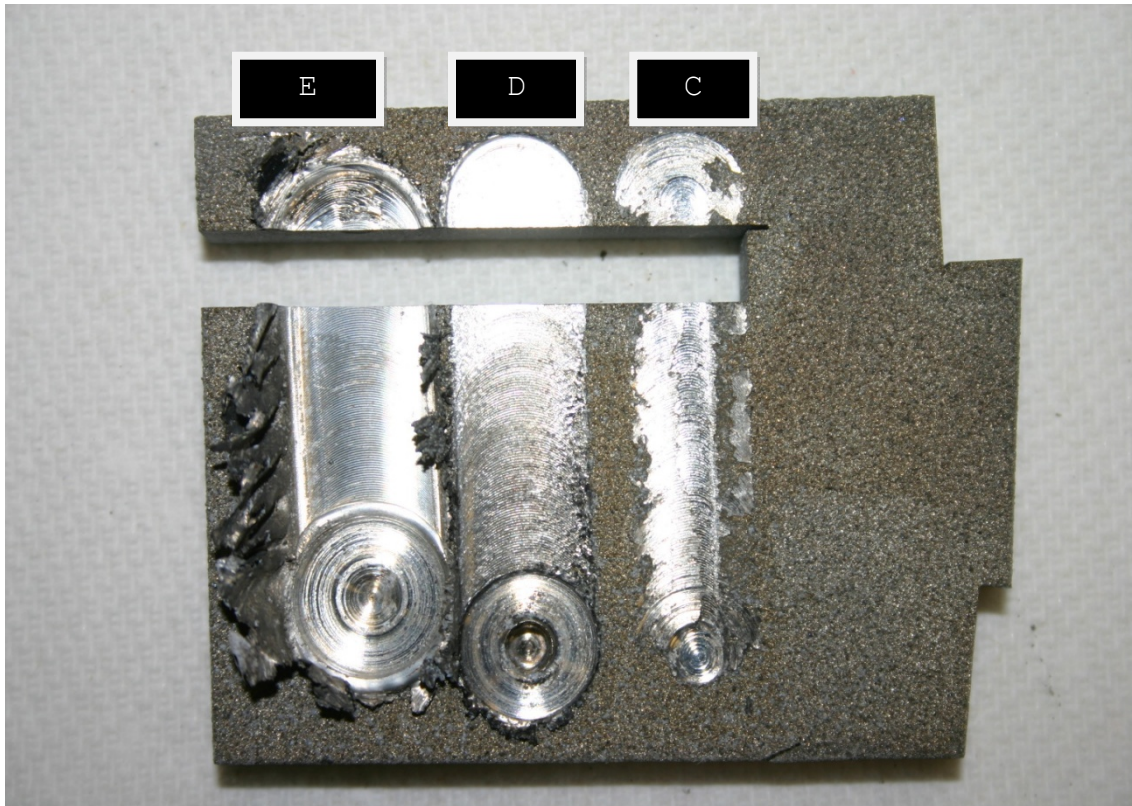


Figure 10. Titanium coated sample showing FSP; D,E: pinned tool single pass FSP, C: Pinless tool FSP; notice the resultant flash on run E. Excessive force led to removal of all Titanium from the surface.

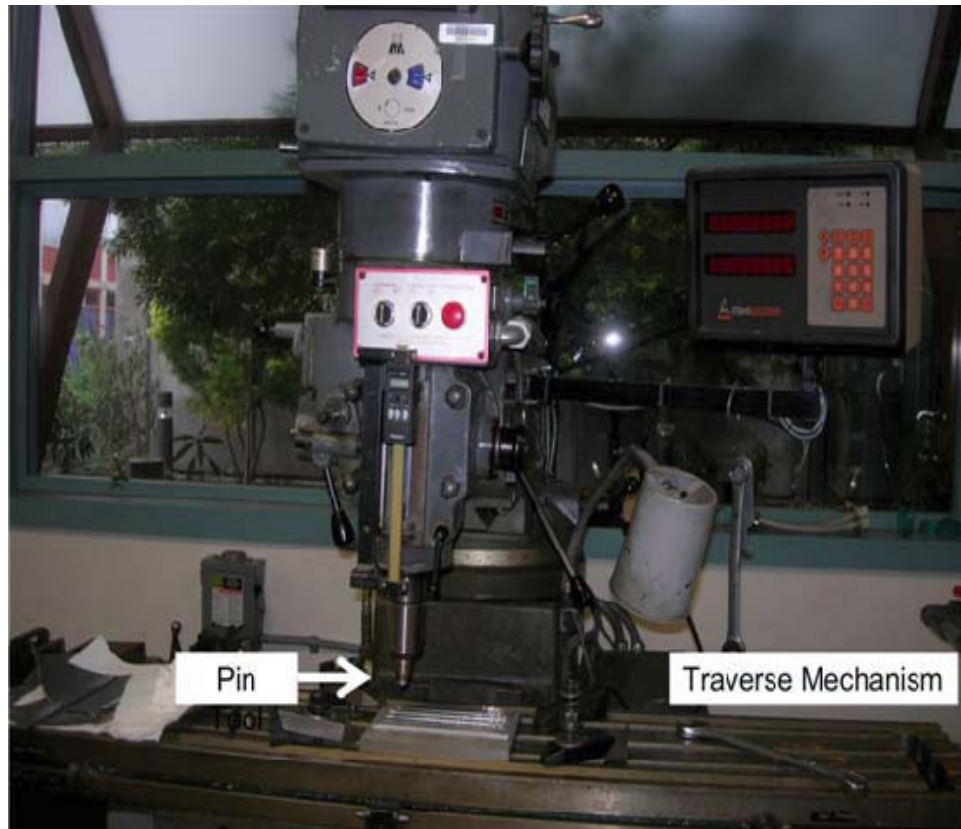


Figure 11. Friction stir processing machinery. From [7].

C MICROSTRUCTURE ANALYSIS

1. Optical Microscopy

a. *Sample Preparation*

Some FSP samples were set into a thermosetting resin that was allowed to mold around the sample and then harden, while other FSP samples were held by hand during the grinding and polishing. Several steps were needed to prepare the samples for optical microscopy, including: mounting some samples, grinding with various grit sand papers, the use of a polishing cloth, and finally, etching. The machine used to grind all of the samples of accomplished by use of a Buehler ECOMET 4 variable speed grinder-polisher. The grinding was done in four steps

using four different Silicon carbide (SiC) sand paper grits. The different papers and speeds are listed below:

Sand paper (grit)	Speed (RPM)
400	160
1200	150
2400	140
4000	120

Table 2. List of sandpaper grit and machine RPM.

After satisfactory completion of grinding, a Buehler ECOMET 3 variable speed grinder-polisher was used. A total of three polishing solutions were placed onto a water wetted Buehler polishing cloth. The first was a 3 micron Buehler MetaDi Monocrystalline Diamond Solution, the second solution is the same with the exception of 1 micron suspended particles versus 3 micron particles, and the third was a Buehler Mastermet .05 micron colloidal silica suspension. All solutions were used at a machine speed of 120-140 rpm. Between each step, samples were rinsed with water, a methanol spray and then heat dried using a hot air gun.

Finally, the samples were etched in preparation for viewing via the optical microscope. The etching solution contained 40 ml of water, 40 ml of ammonium hydroxide, and 2 ml of hydrogen peroxide. Tweezers were used to dip small pieces of cotton swab into the etching mixture, and then swabbed onto the samples. The samples were then rinsed with water, sprayed with methanol, and dried with a hot air gun.

b. Optical Microscopy Procedure

A Nikon Epiaphot 200 optical microscope was used to accomplish the viewing of the polished and etched samples. Micrographs were taken of all samples at various magnification levels ranging from 2.5X-100X. The microstructure of the various sections and zones were photographed via the attached camera.

2. Scanning Electron Microscope

a. Sample Preparation

All samples were examined using a scanning electron microscope (SEM). To facilitate viewing in the SEM sections were cut out of the sample plates. FSP runs A and B were included on one sample, while FSP runs C,D and E were on another sample. In order to achieve thorough conduction, each sample was prepared using a variety of techniques. Silver paste and copper tape was applied to the samples that were set in the resin in order to ensure proper conductivity. The other samples, being metallic in nature, did not need any additional preparation to enhance conductivity.

b. Scanning Electron Microscopy Procedure

All samples were subjected to scanning electron microscopy using a Zeiss Neon 40 SmartSEM Field Emission Scanning Electron Microscope (Figure 13), or the TOPCON SM510 SEM (Figure 12) with a LaB₆ electron gun operating at 15kV. The scanning electron microscope (SEM) was used to analyze all samples and their respective microstructures. Analysis was conducted on the characteristics of the Titanium coating to include: thickness, chemical

composition, porosity, and the presence of cracks. Further analysis was conducted on the base Aluminum to determine the composition and diffusion zone near the FSP surface, and the relative success of consolidating the Titanium coating onto the Aluminum in the stir zones.

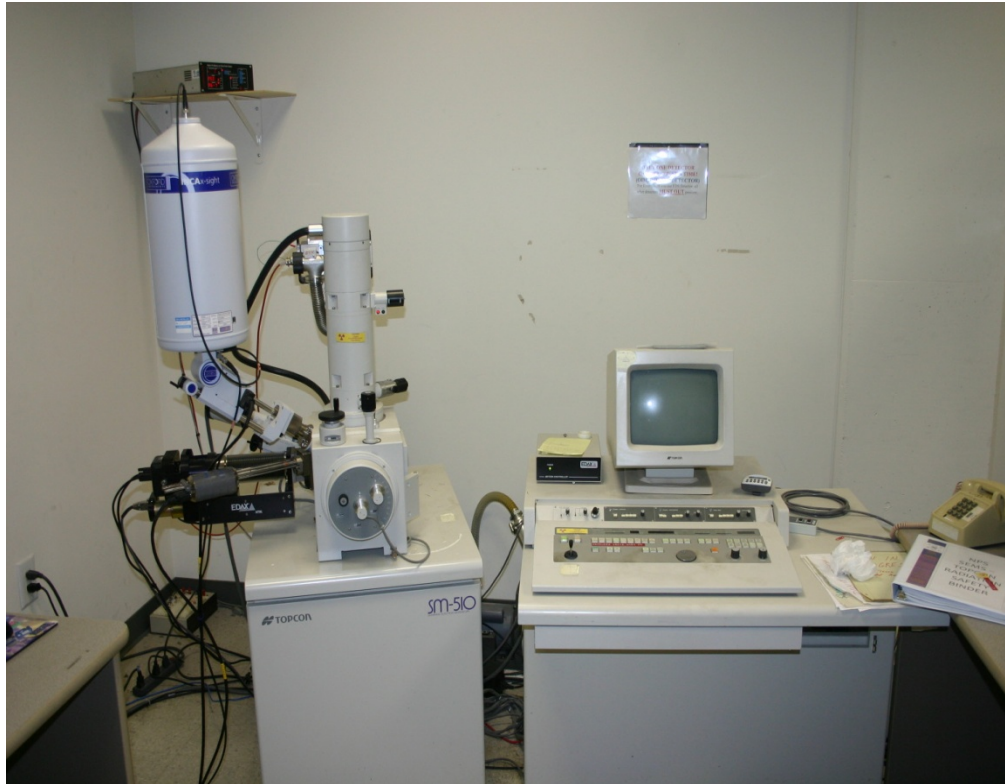


Figure 12. TOPCOM Field Emission SEM.



Figure 13. Zeiss Neon 40 Field Emission SEM.

3. Hardness Data

Hardness measurements were conducted using a Digital Micro-hardness Tester model HVS-1000. The machine allows for various methods of obtaining hardness data; for this experiment, the Vickers hardness scale was utilized. The methodology involved applying a square based-pyramid diamond micro-indenter to the surface of the sample. The applied force was .96 newtons, and the force was held for a dwell time of ten seconds. After removal of the indenter, the diagonals of the diamond shape indentation are measured via the attached microscope and measuring device, while onboard electronics calculated the hardness value, which was displayed on the machine.



Figure 14. Harness testing machine.

THIS PAGE INTENTIONALLY LEFT BLANK

IV. RESULTS

A. OVERVIEW

Aluminum alloy samples were studied to determine the effectiveness of using FSP to consolidate and bond a Titanium based coating onto the base metal Aluminum. Different variations of FSP parameters were used to include: single pass FSP using a pinned tool, Single pass FSP using a pinless tool, multiple pass FSP using a pinned tool, and plunges into the metal with a pinless tool. Results from analysis of optical microscopy, scanning electron, microscopy, and hardness testing are discussed in this chapter.

B. AS PLASMA SPRAYED SAMPLE CHARACTERISTICS

Of particular concern is the fragile nature of the coating upon completion of the plasma spray. Although the coating appears to be very adherent to the base metal, several examples reveal otherwise. As Figure 15 shows, we can see several troubling properties of the untreated sample and its coating. Although most of the Aluminum is coated, there are visible areas that show the exposed base Aluminum, while other areas show very thick sections, as seen in Figures 16 and 17, respectively.

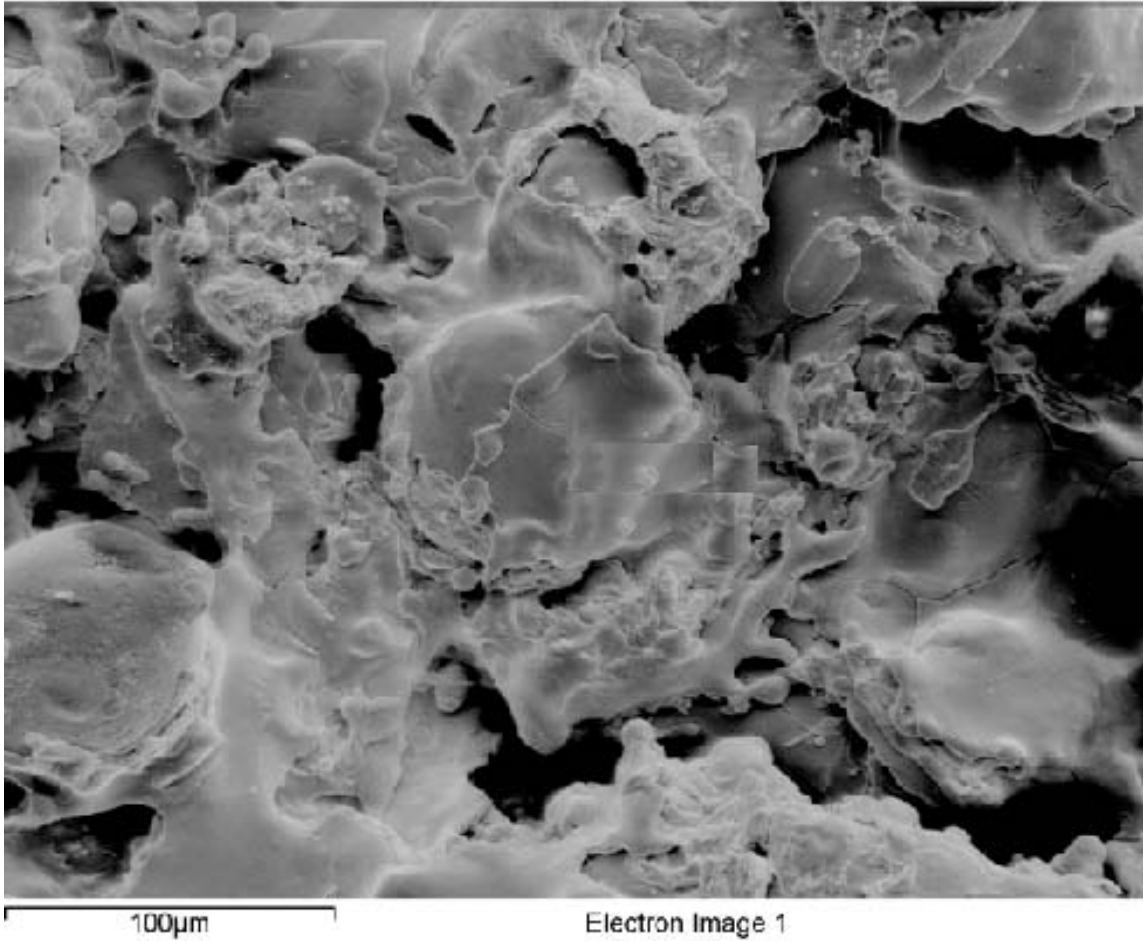


Figure 15. SEM image of plasma sprayed Titanium. Notice the evident voids that form as a result of uneven distribution of material to the surface. Such voids lead to an inherently weaker, and thus, poorly bonded outer layer.

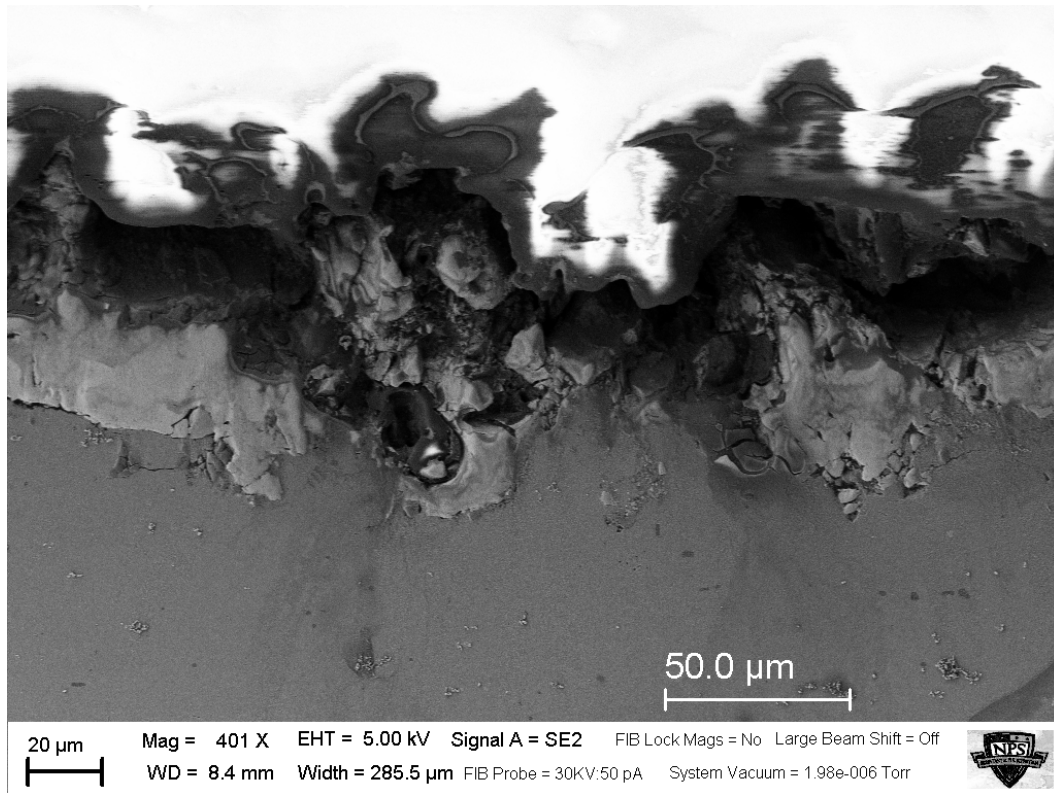


Figure 16. Inconsistent Titanium coating (light gray) leaves the base Aluminum (dark gray) exposed, thereby defeating the purpose of the protective coating. (The very light color at the top is the puck used to mount the sample).

There are several cracks present both in the Titanium coating, and also along the Titanium-Aluminum interface, as seen in Figure 16. These cracks most certainly lead to the flaking and loss of the outer layer due to the lack of strong bonding, especially when the coating is exposed to fast moving debris. As the Titanium breaks off, the base Aluminum is left exposed to the environment.

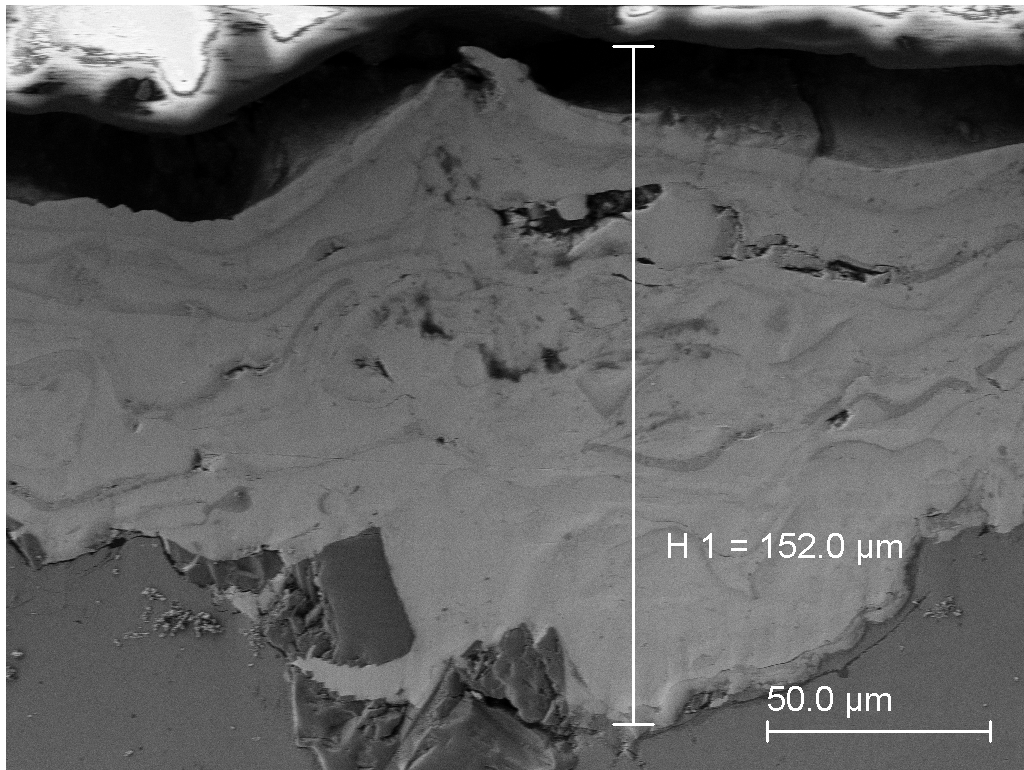


Figure 17. The thickest part of coating measured at over 150 microns; yet the visible voids and cracking at the interface will undoubtedly lead to an overall weaker protective layer.

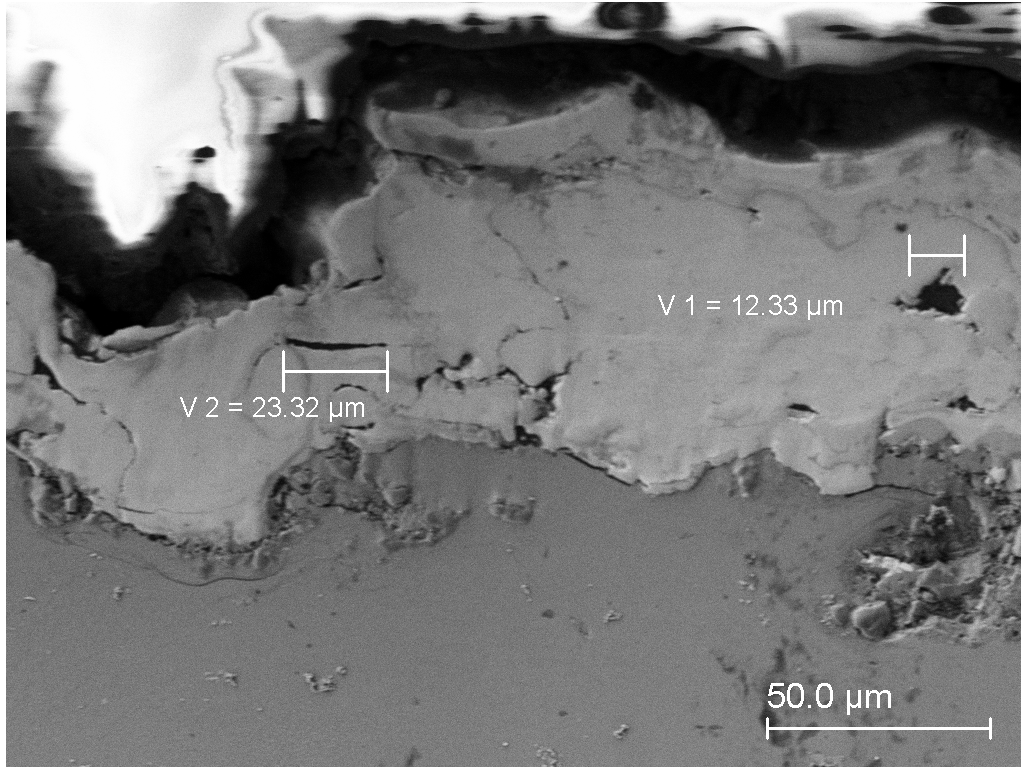


Figure 18. Cracks and pores present before processing contribute to the poor bonding at the interface of the two metals, as well as weakening to the protective coating.

C. MICROSTRUCTURE ANALYSIS

1. Optical Microscopy

The figures below show a low magnification montage of the stir zone A, a single pass pinned tool sample, as well as stir zone B, the multi-pass pinned tool sample. The stir is evident by the apparent shape and change in grain structure.



Figure 19. FSP stir zone A, single pass, pinned tool sample.



Figure 20. FSP stir zone B, multi-pass, pinned tool sample.

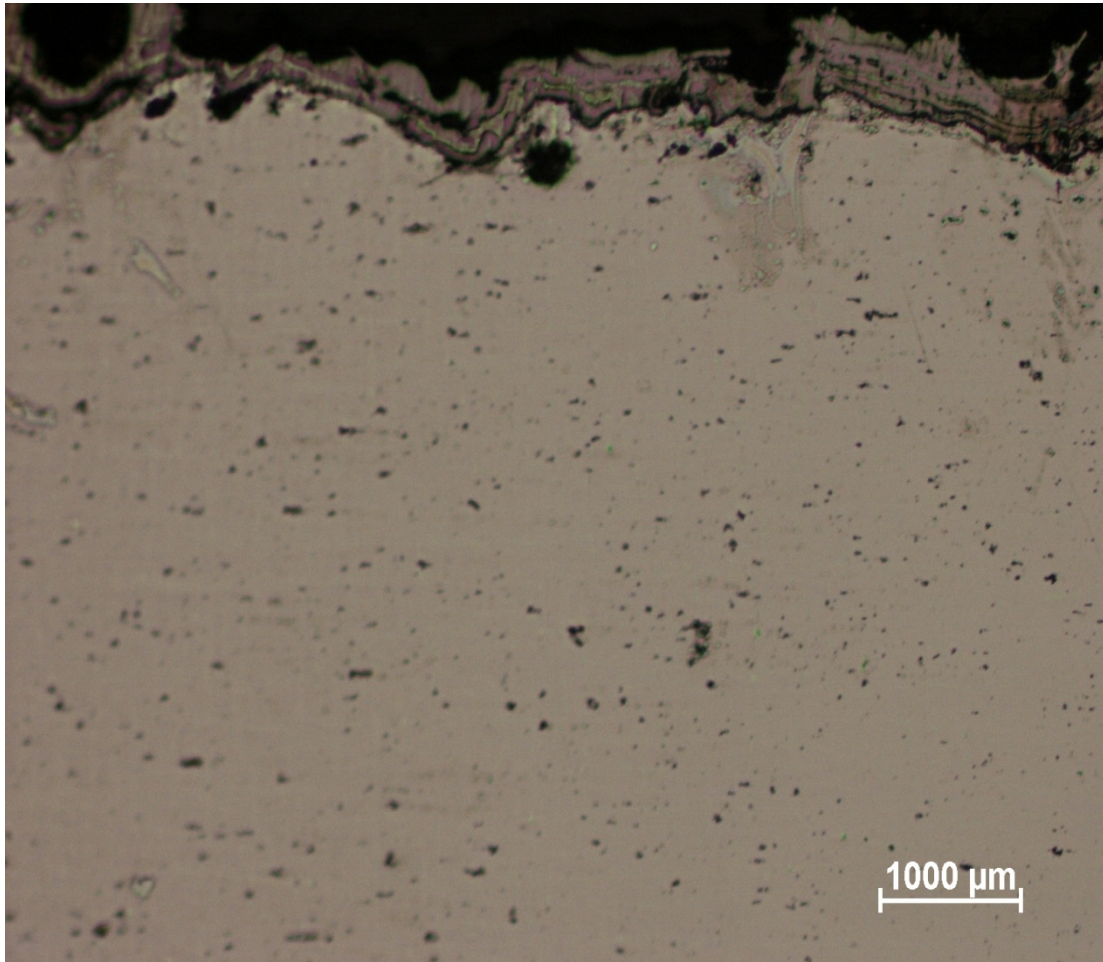
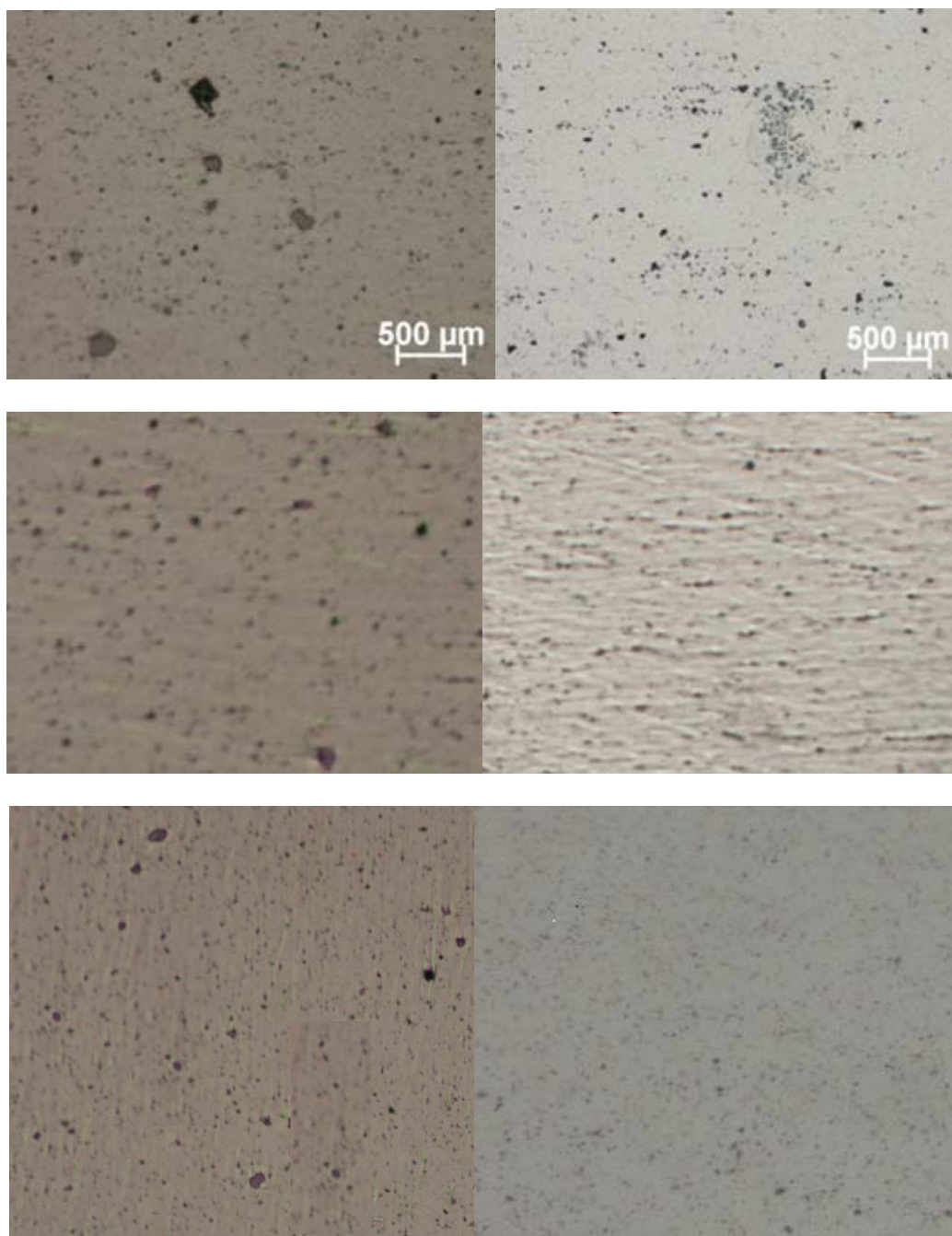


Figure 21. Unprocessed sample shows a random distribution grain structure that is not refined.

The unprocessed sample shows a poorly bonded Titanium layer with the base Aluminum. The coating thickness varies widely across the sample, and severe porosity is noted. Several cracks are present both in the coating, and at the metal to metal interface. The grain structure is random and unrefined.



A

B

Figure 22. Top to bottom: Non FSP region, edge of SZ, middle of SZ; All photos at the same magnification. Notice the Stir Zone's superior mixing and more homogeneous microstructure.

Figures 19-22 show a refinement of the microstructure in the stir zone as a result of the FSP. The average grain size has been reduced, and the coating has been partially consolidated, but not in a particularly useful way. Run D yielded similar results, but too much downward force was applied during the FSP, and the end result was the removal of the Titanium coating. Runs C and E were done with a pinless tool, so no obvious stir zone was found.

2. Scanning Electron Microscope

Analysis was conducted via SEM in order to resolve microstructure characteristics that could not be accomplished on the optical microscope. The SEM allows not only for more detailed photographs, but also for use of EDS technology. Utilizing EDS data will allow for analysis of surface composition, the basis of this research, and also allows for the analysis to determine the amount of mixing that may be occurring at the interface of the protective layer and the base alloy.

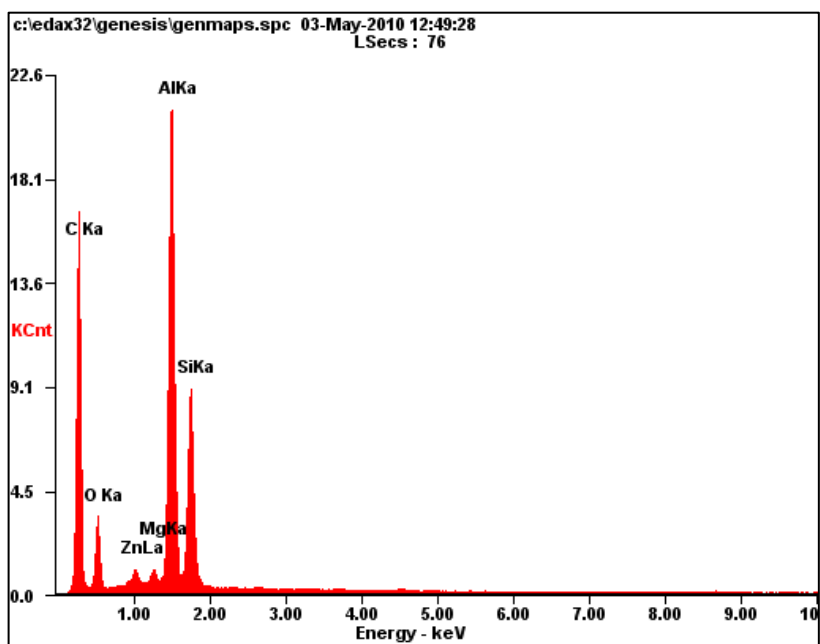
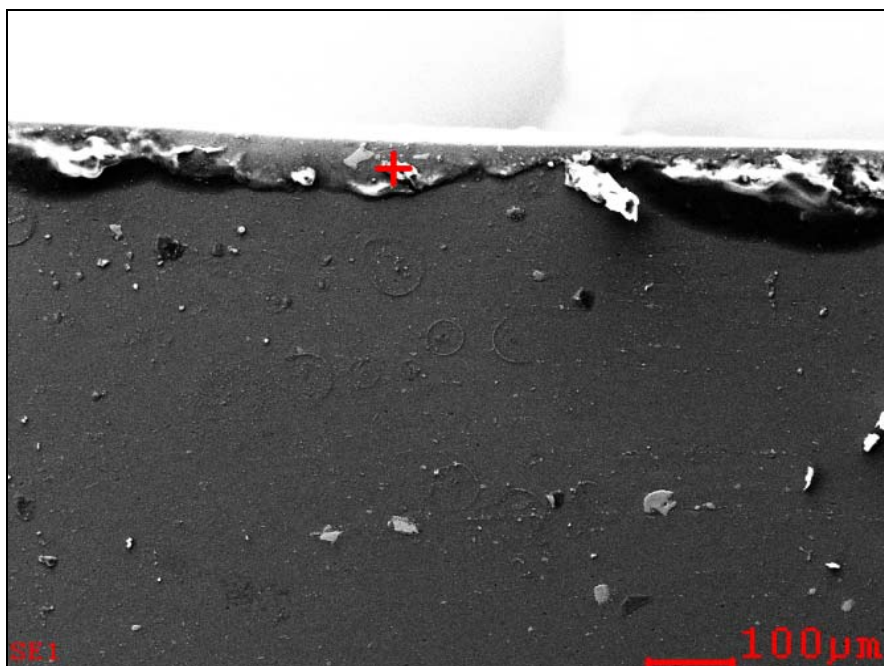


Figure 23. Stir Zone A: Secondary electron image (top) showing that there is very little or no Titanium coating on the surface of the sample in the stir zone area. Xray spectrum from the area marked + in the image shown (bottom). There is no evidence of Titanium in the region. Titanium K_{α} line is expected at 4.51keV.

The image above shows that the FSP was unsuccessful in consolidating the Titanium layer into the Aluminum, as EDS shows virtually no Titanium in the stir zone. During the single pass FSP run with the pinned tool, almost all the Titanium coating spalled off (as seen in Figure 13) and very little Titanium was incorporated into the Aluminum alloy. This presumably occurred due to the high downward force applied during the FSP process with the pinned tool. One can also propose that more than one pass of FSP is necessary in order to achieve adequate mixing, and that is supported by Figure 24.

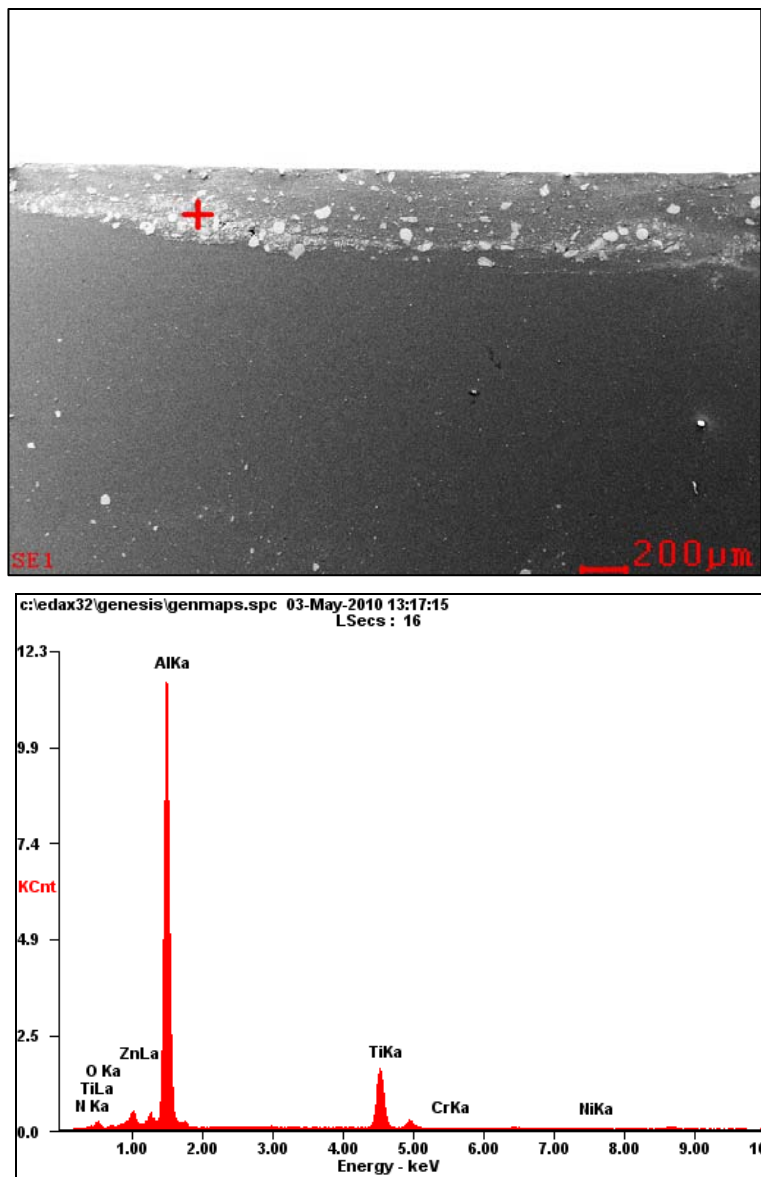


Figure 24. Stir zone B secondary electron image (top, taken in the vicinity of the + on the image) shows some consolidation between the broken up Titanium particles (light gray) and the base Aluminum (dark gray). Xray spectrum (bottom) shown the expected 4.51keV Titanium K_{α} line.

It was observed that during the multipass FSP (experiment B) some quantity of the Titanium coating spalled off during the first pass and was incorporated into the Aluminum during subsequent passes. This is demonstrated in Figure 24.

These results are mixed but promising. The surface layer is a mix of Titanium and Aluminum, and the consolidation layer extends approximately one half of a millimeter in the base. Hardness data supports the consolidation (see Figure 32), as hardness values down to a depth of .3 mm are nearly double that of the base Aluminum, while only about 25% less than the hardness of the Titanium based coating.

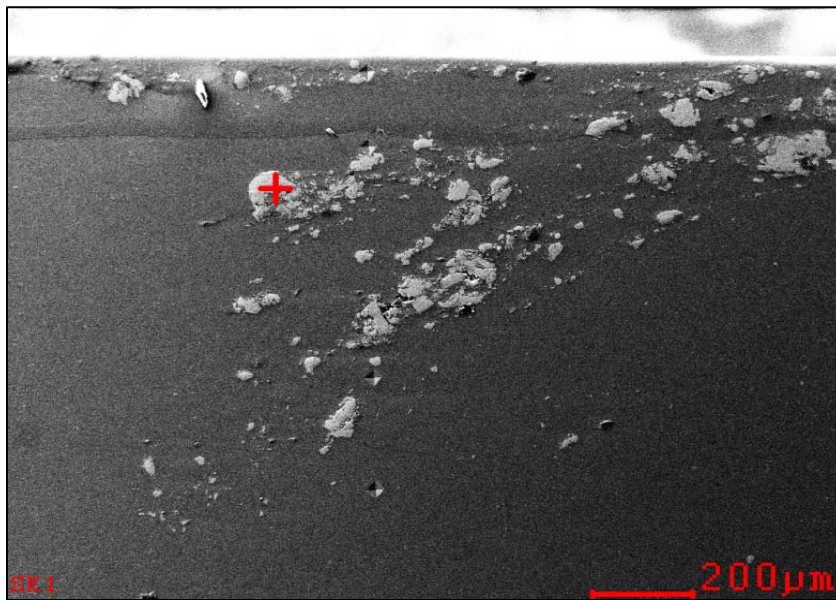


Figure 25. Stir zone D: The dark base is the Aluminum, the lighter the Titanium; Notice the barley present titanium is no longer on the surface as protection.

Stir zone D is shown in Figure 25, and although this was a single pass run, again the results suggest that the coating layer may be incorporated into the base metal. We see a partially consolidated Titanium-Aluminum mixture, though not nearly as mixed as stir zone B. Instead, we see several large pieces of the Titanium layer that has been broken up and dispersed into the base, to a depth of nearly

.75 mm. Once again, this leads us to believe that a single pass may not be adequate for sufficient mixing.

Stir zones C and E did not provide any significant results. For both runs, too much downward force resulted in no Titanium being left on the surface at the completion of the FSP.

After finishing the single pass and multi-pass FSP runs with the pinned tool, a design was made for a pinless tool. Upon receipt of the pinless tools, plunges (with no traverse) were made into the same samples, and the results are discussed now.

There were two different sets of plunges made into the material. As shown in Figure 12, plunges I and IV were the most successful, as our tools failed and left material on the sample in plunges II and III. Plunge I was most successful as Titanium was still present on the surface, where there was very little Titanium left on plunge four.

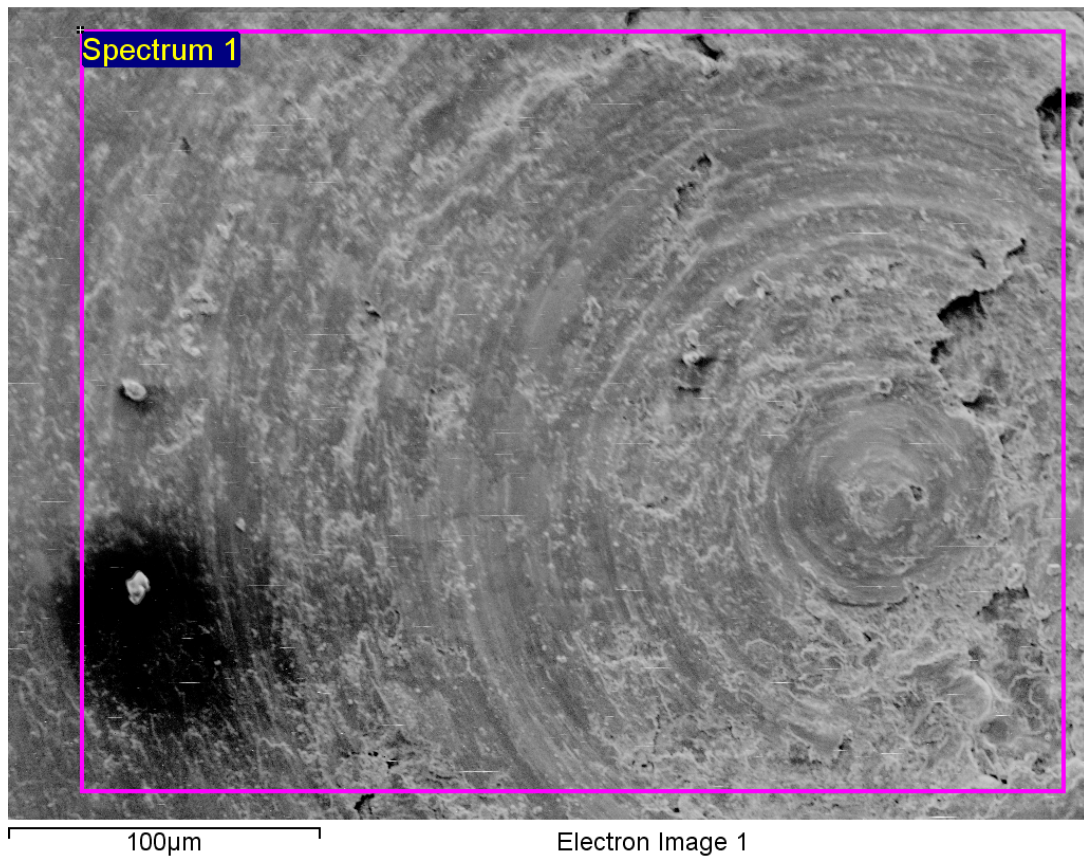


Figure 26. SEM photo of plunge area I; The lighter “white” material is the Titanium, while the darker Aluminum base makes up the majority of material.

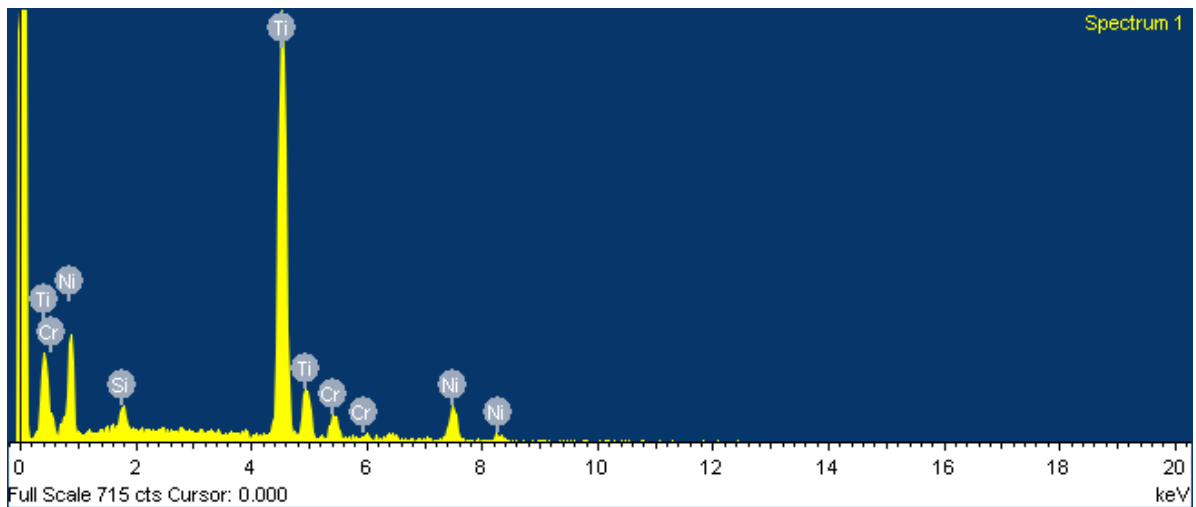


Figure 27. EDS data of plunge area I; Titanium still present on the surface.

Hypothesizing that too much downward force was being used, a second set of plunges was then devised. This time, paying very close attention to plunge force, we were able to achieve much better results. We plunged at RPMs of 400, 800, and 1500, each delivering results that are superior to the first round of plunges. Keep in mind, the overall goal is to modify the existing Titanium coating such that porosity is improved, as well as the bond between the coating and the substrate.

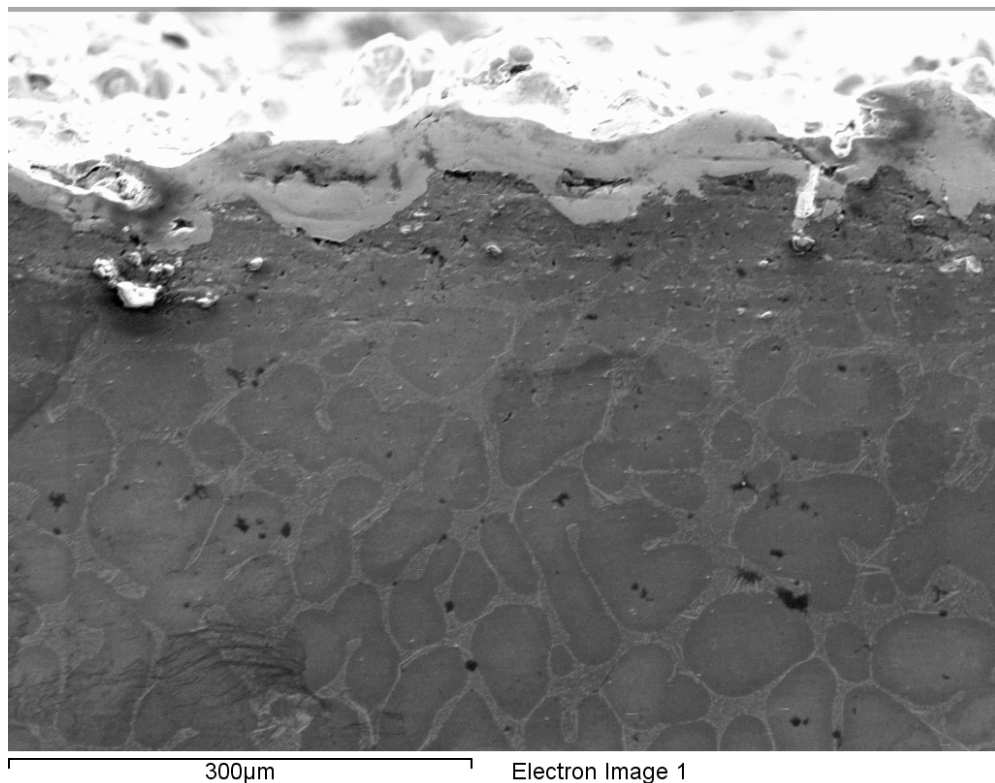


Figure 28. As cast Aluminum-Silicon alloy micrograph.

One can easily see that porosity both in the Titanium layer and at the bond interface is greatly improved, by comparison of Figures 28 and 29. Although this experiment

involved only a plunge, the next logical step was to test out various other RPMs to see if such satisfactory results could be duplicated.

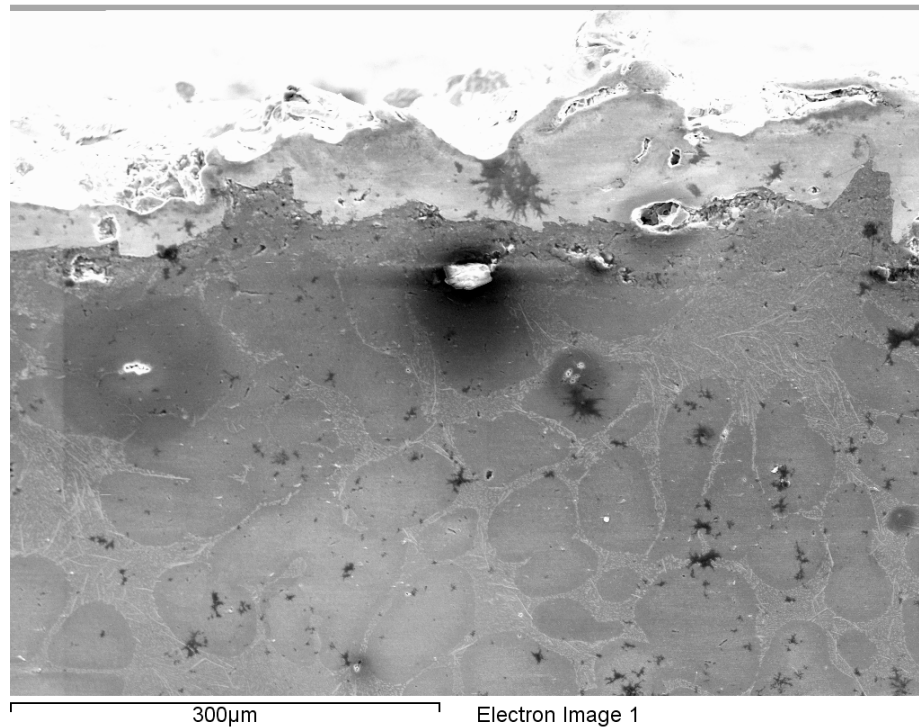


Figure 29. 1500 RPM plunge showing the intact Titanium layer and the much improved porosity, with very little mixing of the Titanium and Aluminum.

Upon initial observation, the 1500 RPM sample looks to be more impressive than the 400 RPM sample. Further investigation revealed that when FSPing a hard metal such as Titanium, published results show that in many cases an elevated RPM was used, usually between 1000-2500 RPM, thus verifying what we see in Figure 29.

The last experiment to be performed was that of a pinless tool traverse. The overall goal was to take the progress that had been observed in the simple plunges and see if that success could be applied to a full plunge and

traverse. Again, the RPM was 800, the IPM was four inches per minute, and although the downward force was not measured directly, it was extremely light. The methodology was to bring the rotating tool down until contact was just beginning, and then to begin the traverse.

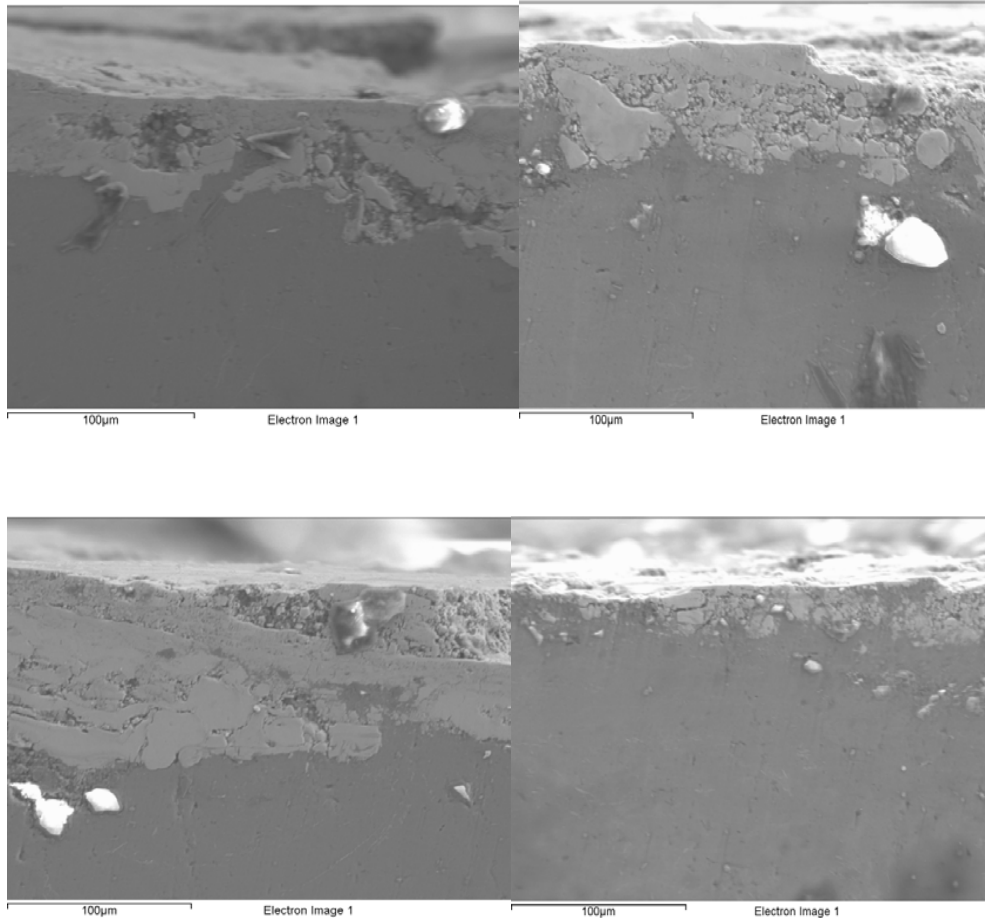


Figure 30. SZ of the flat tool FSP run shows much less porosity that the as plasma sprayed sample or the pinned FSP experiments. Along with reduced porosity, there is very little evident separation at the Titanium-Aluminum interface.

One of the most obvious results is the lack of porosity at the Titanium-Aluminum interface. Although this is not conclusive proof that the interface bond is stronger, one could hypothesize such, but further testing is in order. Also of interest is the fact that the Titanium coating is still present on the surface. One of the early challenges with the pinned tool was the undesirable consolidation of the protective coating with

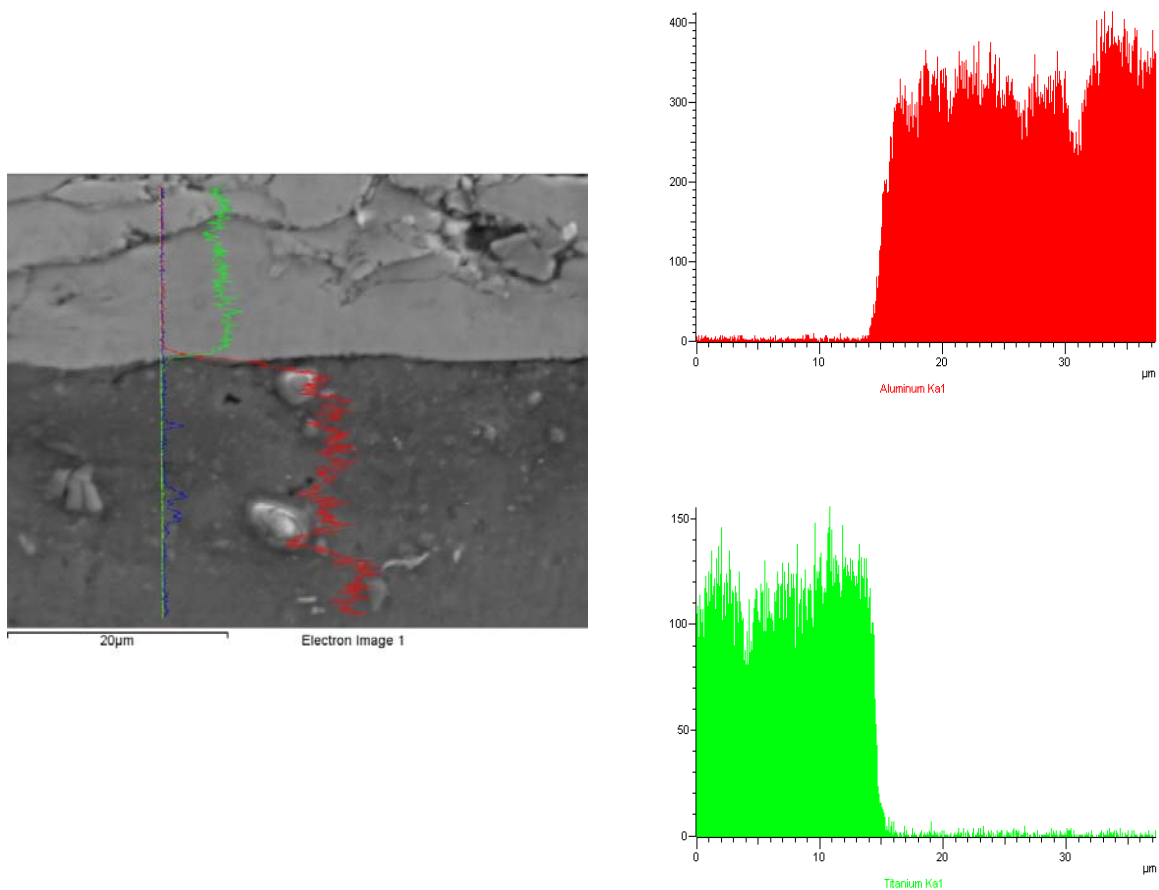


Figure 31. Line scan of the flat tool FSP run; Aluminum shown in red, Titanium shown in Green. The line scan shows in addition to reducing porosity and minimizing cracks at the interface, very little mixing occurs between the Titanium and the Aluminum, demonstrating successful treatment of the surface layer while minimally affecting the base metal.

D. HARDNESS DATA

Of particular interest is the hardness of both the Titanium layer and the hardness profile in the stir zone. For the pinless plunges and runs, a change in hardness of the Titanium layer would be anticipated, and perhaps the interface area as well. With a pinned traverse, due to the

presence of the pin and thus the deeper penetration, we hope to see an increased hardness profile extending into the stir zone.

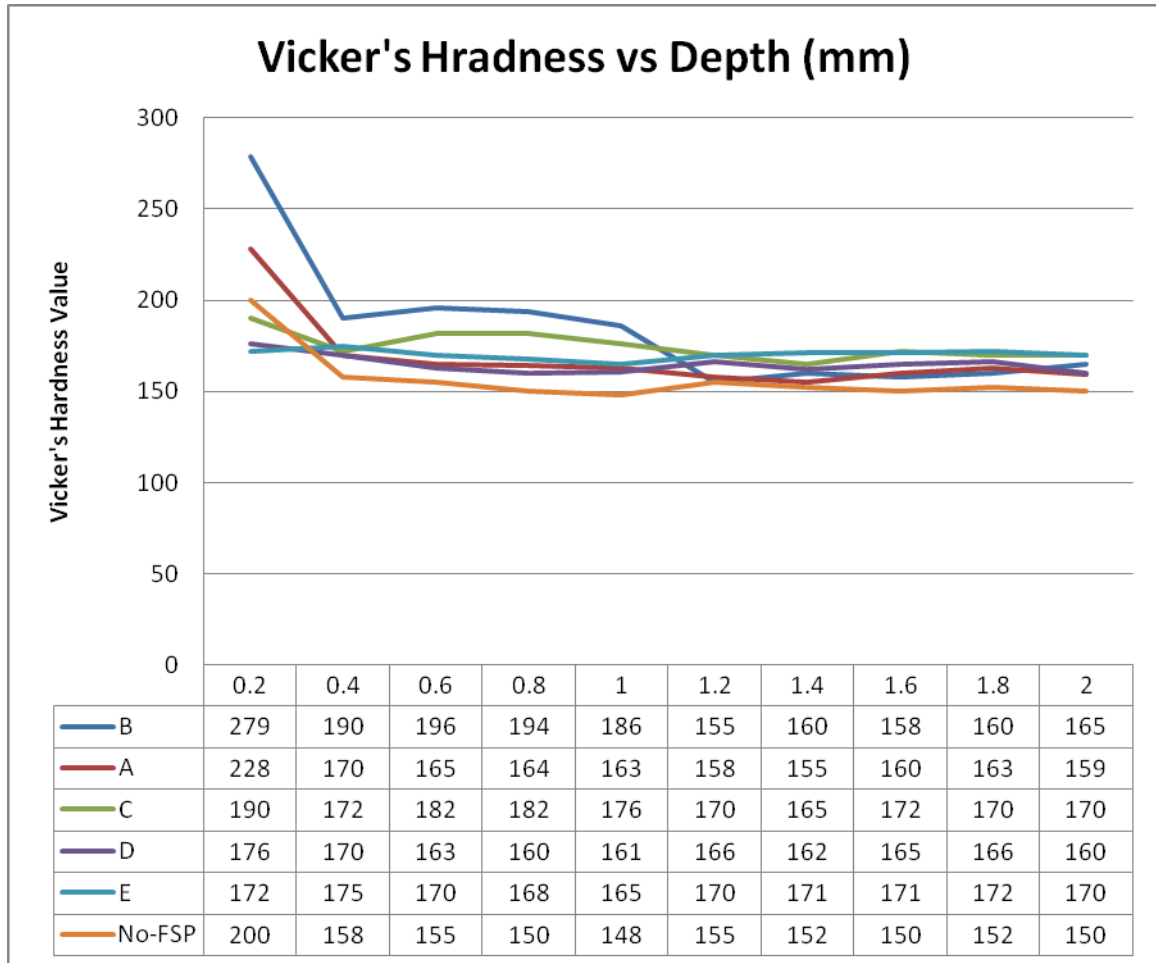


Figure 32. A graph of Vickers hardness vs Depth (in mm). As expected, FSP of a metal leads to increased hardness, partly by refining and homogenizing the microstructure. Increased hardness was observed in both the Titanium and the Aluminum.

THIS PAGE INTENTIONALLY LEFT BLANK

V. DISCUSSION

Comparison between the FSP material and non-FSP samples reveal that the FSP process consistently delivers a homogenous, refined microstructure. Although a pinned, single pass is able to partially consolidate the Titanium coating into the Aluminum, the pinned multiple pass FSP was much more successful. The multiple pass FSP seems to provide much better mixing in the SZ, achieving much better homogeneity. Several passes would need to be made if a full consolidation of the surface and the substrate is to be achieved.

After further review, it became evident that consolidation of the surface layer and the base may not be the best solution, as shown below, adequate alloying was not able to be achieved, even with three passes.

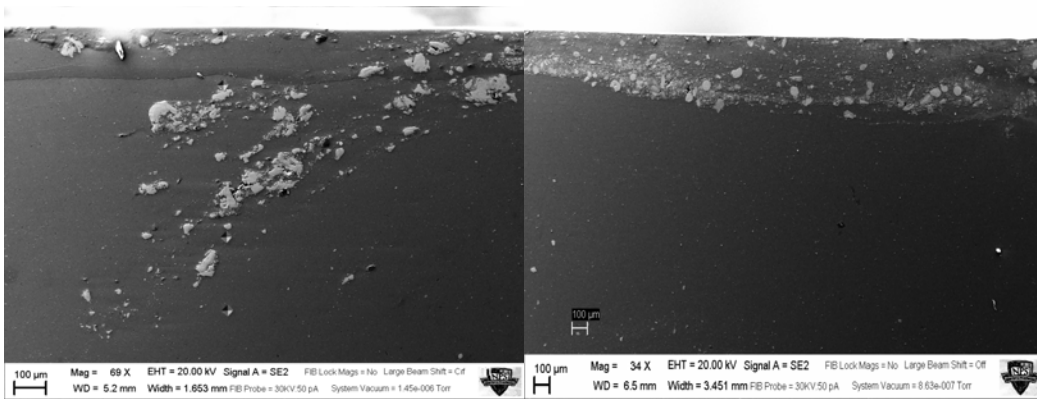


Figure 33. Scanning electron image of: Single pass (left) versus multiple pass (right) surface consolidation. The multipass mixing is far superior and yields a more homogenized particle distribution. (Light gray particles are the Titanium).

More successful, however, was the flat tool FSP, as the coating appeared to be more consistent in depth, contained significantly less porosity, and seemed to have fewer cracks at the Titanium-Aluminum interface, which will prove to be key if adhesion of the protective layer is to be improved. One could further hypothesize that multiple flat tool runs of the same sample would provide the mechanism needed to even further process the Titanium, and increase bonding between the Titanium and Aluminum.

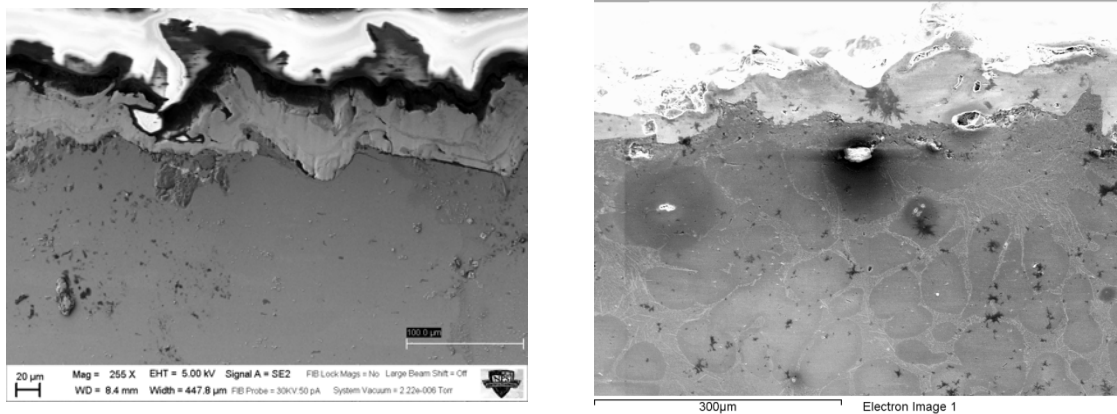


Figure 34. Scanning electron image of: Unprocessed material before (left) and after (right) flat tool FSP. FSP material consistently shows reduced porosity, less cracking at the interface, and a more even Titanium distribution along the surface.

Of particular importance is the combination of parameters that can achieve the best results. Of course, due to time constraints, not every set of RPM, IPM, pinned or pinless tool, pin size, pin shape, and downward force could be attempted. In fact, only a small fraction of possibilities has been tried in this endeavor. One important point to mention is the lack of a downward force

measuring device that was available for use during the traverse. Although fabrication of such a device has been started, no such device was used during any of the experiments; the use of such a device would be invaluable for any future experiments.

Also of note was the effect that the FSP had on the hardness of the samples. The increase in hardness is an expected and documented advantage of the friction stir process itself. As the tool passes through the material, grain sizes become smaller, homogenous, and refined, resulting in the increased hardness. As of this writing, no hardness data is available for the second round of flat tool plunges, or the flat tool traverse, due to the department's hardness machine being out of commission.

THIS PAGE INTENTIONALLY LEFT BLANK

VI. CONCLUSIONS

This thesis reports the first preliminary experiments aimed at consolidation of a relatively hard and porous plasma sprayed coating on Aluminum alloys by FSP. The objective was to examine various FSP tool geometry and processing conditions that will result in producing adherent non-porous hard surface coatings on alloy surfaces. The main conclusions from this study are:

1. Conventional FSP processing parameters (RPM/IPM combinations) with a pin tool appears to quickly dislodge the porous coating from the surface.

2. Multiple pass FSP with a pinned tool showed promising results regarding the consolidation of the Titanium layer and Aluminum base.

3. Flat tool FSP results were far superior to both the pinned tool and the pinless tool traverses. Achieved were greater surface layer consolidation, reduced surface layer porosity, and better contact at the surface layer-base interface.

4. All pinned FSP samples saw a refined, homogenous microstructure as a result of the FSP technique.

5. Hardness values were raised in all instances, even if the Titanium later was removed during the processing.

6. A device capable of measuring plunge force during the traverse will be needed in order to achieve desired, repeated results with concerning the flat tool traverse.

THIS PAGE INTENTIONALLY LEFT BLANK

VII. RECOMMENDATIONS FOR FUTURE WORK

1. Develop a method for measuring the downward plunge force, and ensure that this force can be measured during the traverse.

2. Perform FSP traverses using different combinations of RPM, IPM, and plunge force.

3. Perform more FSP using the flat tools. Be sure to include single pass and multiple pass traverses.

4. Investigate hardness values of both the surface metal, and the base metal that result after the flat tool FSP.

5. Investigate the same procedures using different surface metals and base metals.

THIS PAGE INTENTIONALLY LEFT BLANK

LIST OF REFERENCES

- [1] TWI Technology Engineering. 2010. "Friction Stir Welding at TWI." LWI Ltd. Cambridge, UK, <http://www.twi.co.uk/content/fswintro.html>; Accessed April 2010.
- [2] Anderson, T., 2010, "ESAB Welding and Cutting Education." Esab Inc., Florence, SC, <http://www.esabna.com/us/en/education/knowledge/qa/what-is-friction-stir-welding-of-aluminum.cfm>; Accessed May 2010.
- [3] Z.Y. MA, 2008, "Friction Stir Processing Technology: A Review," *Metallurgical and Material Transactions*; vol. 39, pp. 642-658.
- [4] Morisada, Fujii, Mizuno, Abe, Nagaoka, Fukusumi, 2010, "Modification of Thermally Sprayed Cemented Carbide Layer by Friction Stir Processing," *Surface & Coatings Technology*, v. 204; pp. 2459-2464.
- [5] Rhodes, Mahoney, Bingel, Calabrese, 2003, "Fine-grain Evolution in Friction-stirred Processed 7050 Aluminum," *Scripta Materialia*; vol. 48; pp. 1451-1455, .
- [6] Kwon, Shigematsu, Saito, 2003, "Mechanical Properties of Fine Grained Aluminum Alloy Produced by Friction Stir Process," *Scripta Materialia*; vol 49; pp. 785-789.
- [7] Santell, Engstrom, Storjohann, Pan, 2005, "Effects of Friction Stir Processing on Mechanical Properties of the Cast Aluminum Alloys A319 and A356," *Scripta Materialia*; vol. 53; pp. 201-206.
- [8] Mishra, Mahoney, McFadden, Mara, Mukherjee, 2000, "High Strain Rate Superplasticity in a Friction Stir Processed 7075 Al Alloy," *Scripta Mater*, vol. 42; pp. 163-168.

- [9] Mishra, Ma, Charit, 2003, "Friction Stir Processing: A Novel Technique for Fabrication of Surface Composite," *Material Science and Engineering*; vol. A341; pp. 307-310.
- [10] Elangovan, Balasubramanian, 2007, "Influences of Pin Profile and Rotational Speed of the Tool in the Formation of Friction Stir Processing Zone in AA2219 Aluminum Alloy," *Material Science and Engineering*; vol. A459; pp. 7-18.
- [11] Rhodes, D., 2010. "Keys to Metal Product Fact Sheet." Keys to Metals, AG, St Louis, MO, <http://www.keytometals.com/page.aspx/AluminumProperty.html>; Retrieved May 2010.
- [12] Alcoa, 2010. "Alcoa Alloy 7075 Product Data Sheet." Alcoa Inc., Pittsburgh, PA, http://www.alcoa.com/gcftp/catalog/pdf/alcoa_alloy_7075.pdf; Retrieved May 2010.
- [13] TSET. 2010. "Technology of Surface Texturing." TSET Inc. Santa Clara, CA, <http://www.tosohset.com/ceramiccoat.htm>; Retrieved July 2010.
- [14] Yon, M., 2010. "The Kopp-Etchells Effect." <http://www.michaelyon-online.com/the-kopp-etchells-effect.htm>. Retrieved June 2010.
- [15] Hayashi, J. T. 2009. "*Friction Stir Processing of As-cast Al5058: Super-plastic Response*", M.S. Thesis, Naval Postgraduate School, Monterey, CA.

INITIAL DISTRIBUTION LIST

1. Defense Technical Information Center
Ft. Belvoir, Virginia
2. Dudley Knox Library
Naval Postgraduate School
Monterey, California
3. Engineering and Technology Curricular Office, Code 34
Department of Mechanical and Aerospace Engineering
Naval Postgraduate School
Monterey, California
4. Professor Terry R. McNelley, Code ME/Mc
Department of Mechanical and Aerospace Engineering
Naval Postgraduate School
Monterey, California
5. Professor Sarath Menon
Department of Mechanical and Aerospace Engineering
Naval Postgraduate School
Monterey, California